HHS Public Access

Author manuscript

Mater Sci Eng C Mater Biol Appl. Author manuscript; available in PMC 2023 July 25.

Published in final edited form as:

Mater Sci Eng C Mater Biol Appl. 2019 December ; 105: 110070. doi:10.1016/j.msec.2019.110070.

Electrospray for generation of drug delivery and vaccine particles applied *in vitro* and *in vivo*

Rebeca T. Steipel[a], **Matthew D. Gallovic**[b], **Cole J. Batty**[a], **Eric M. Bachelder**[a], **Kristy M. Ainslie**[a,c,d,*]

[a]Division of Pharmacoengineering and Molecular Pharmaceutics, Eshelman School of Pharmacy, University of North Carolina at Chapel Hill, USA

[b]IMMvention Therapeutix, Durham, NC, USA

[c]Joint Department of Biomedical Engineering, University of North Carolina at Chapel Hill/North Carolina State University, USA

[d]Department of Microbiology and Immunology, University of North Carolina at Chapel Hill, USA

Abstract

Also known as electrospray, electrohydrodynamic atomization has been used extensively in the last 15 years to develop polymer-based particles for drug delivery in cell and animal models. More recently, novel core-shell, multi-axial, and other electrospray particles have been developed from an array of polymers for a variety of biomedical applications. This review focuses on electrospray as a novel method of particle fabrication for drug delivery, specifically highlighting the applications of these particle systems in cell culture and animal models while also discussing polymers used for particle fabrication. Applications of electrospray particles to treat glioma, ovarian cancer, and breast cancer are reviewed. Additionally, delivery of antibiotics, gene therapy, and bacterial cells formulated in electrospray particles is discussed. Finally, vaccines as well as drug eluting particles for differentiation of stem cells and tissue engineering are highlighted. The article concludes with a discussion of where the future of electrospray technology can go to strengthen its foothold in the biomedical field.

Keywords

Polymeric particles; Cancer; Antimicrobial; Gene delivery; Cell delivery; Vaccines; Tissue engineering

1. Introduction

Electrospray (ES), also known as electrohydrodynamic atomization, has emerged as an advanced technology to generate particles for drug delivery. ES is akin to electrospinning, but is usually performed with more dilute polymer solutions while using the same experimental setup: a high-voltage power source, a glass syringe, a syringe pump, and a

*Corresponding author at: Marsico Hall 4211, 125 Mason Farm Road, Chapel Hill, NC 27599, USA. ainsliek@email.unc.edu (K.M. Ainslie).

grounded conductive surface [1] (Fig. 1a). Moreover, ES has the versatility to produce particles comprised of polymers [2,3], microbubbles [4], polyplexes [5], amphiphilic polymers [6,7], silica [8], and lipids [9,10]. These particles have been used for the encapsulation of small molecules, proteins, theranostic elements, nucleotides, cells, and other therapeutics [2,7]. In addition, polymeric particles have been shown to encapsulate multiple elements as well as incorporate multiple polymers to form di-, tri-, tetra-, and additional layered polymeric particles [2].

Typically, ES involves the generation of an aerosol spray of the cargo(s) and encapsulant matrix(es). Using a syringe pump at a low flow rate of hundreds of microliters per hour, a volatile solution with the matrix(es) and encapsulate(s) dissolved is sprayed through a needle onto or into a solid or liquid substrate. Applying positive or negative charge to the needle or collection substrate in order to create a difference in electrical potential on the order of tens of kilovolts (kV) results in the formation of a Taylor Cone at the needle orifice. In a monoaxial (single needle) spray, all of the sprayed constituents mix throughout the process; however, in a multi-axial spray (Fig. 1), the individual solutions (*e.g.* protein in aqueous phase and polymer in an organic solvent) do not mix until they leave their respective channels in the syringe needle and enter the Taylor Cone (Fig. 1a). This limited mixing can facilitate the formation of core-shell particles wherein an inner core particle is formed with an outer layer around it [13]. At the tip of the Taylor Cone the solution is ejected in a jet toward the oppositely charged collection substrate. At relatively high polymer concentrations, polymer chain entanglement results in high viscosity of the solution, such that the Taylor Cone jet forms a continuous fiber travelling to the collection substrate, known as electrospinning. At lower solution viscosities, aerosol droplets are ejected due to repulsion forces that are an effect of like charges overcoming the cohesive forces of surface tension and viscosity, resulting in an electrospray. Maintenance of a stable spray requires balancing the solution properties with the flow rate, along with a number of other parameters (Fig. 2). After the droplets are aerosolized, they travel to a grounded or oppositely charged conductive plate or liquid where they collect. As the droplets move toward the substrate, the volatile solvent carrier evaporates, increasing the droplet charge density and leading the droplets to split into even smaller droplets, which increases the overall droplet surface area and leads to rapid evaporation of solvent over a relatively short distance. The effect of this evaporation on the particle morphology can vary according to the ratio of the rate of evaporation to the rate of solute diffusion within the solvent, which can be represented as the Peclet number [14]. A low rate of diffusion of the solutes through the droplet, corresponding to a higher Peclet number, results in accumulation of solutes at the surface of the droplet as the solvent evaporates, leading to the formation of a hollow droplet which eventually crumples or collapses into a toroid or wrinkled particle shape. Higher rates of diffusion, corresponding to a lower Peclet number, allow solutes to reequilibrate to a more energetically favorable homogenous spherical distribution, resulting in the formation of more smooth particles [15]. At times, an increase in the temperature of the air surrounding the spray, *via* heat lamp or other system, is used to fully evaporate the solvent. If the solvent is not fully evaporated at time of impact on the grounded plate, the particles will aggregate and/or flatten. Temperature, distance to plate, flow rates, viscosity, charge, salt concentration of solutions, solvent used, and numerous other variables can be finetuned to

optimize particle production and vary morphology. These factors can lead to complex and novel particles that can have several benefits.

No matter how the particles are formed, or the cargo incorporated, there are several benefits to the generation of nano/microparticles using ES, especially in comparison to other common polymeric particle fabrication techniques such as emulsion, coacervation, or even microfluidic devices. The generation of particles *via* ES can lead to a less polydisperse size population than other methods, while minimizing batch-to-batch variation [9,10,13]. Additionally, compounds with a broader range of partition coefficients can generally be accommodated with ES since mono- or multi-axial generation of particles facilitate the use of a range of solvents and aqueous solutions individually or cosprayed. In addition, emulsification prior to spraying has been reported, which could further expand the number and types of cargoes that can be used [17]. Better solubility of the cargo in addition to using a continuous phase of air, rather than water or another solvent, leads to another advantage of ES: high encapsulation efficiencies (EEs) [18]. Whereas compounds can partition into the continuous aqueous phase during standard emulsion methods, in ES the spray aerosol is generated into air, limiting the ability of the cargo to diffuse away. Having a high EE facilitates facile encapsulation of multiple agents at a controlled amount (*e.g.* ratio to each other) that is often difficult to achieve with other methods where the inclusion of multiple agents may affect the EE of individual agents [11,19]. Another benefit is that the scalability of ES is improved compared to emulsion and coacervation processes because it is a continuous rather than batch method that scales linearly with the number of ES heads [20,21]. This scalable production has been applied in materials coatings and can be advantageous when developing low cost therapies and vaccines. The importance of production cost is illustrated by the limited advancement of poly(lactic-*co*-glycolic acid) (PLGA) tetanus vaccines by the World Health Organization (WHO), in part because production costs were too significant [22]. Another aspect of the limited advancement of PLGA tetanus vaccines was the denaturation of the protein antigen during the emulsion process, not only due to prolonged contact with the solvent, but also the high-speed shearing during emulsion. Proper protein tertiary and perhaps even quaternary structure is important in both protein therapeutics and for B cell activation in vaccines [23]. ES has been shown to be less harsh on proteins compared to methods like emulsion because it uses low shear forces and minimal contact time with solvents, on the order of microseconds in the Taylor Cone during a co-axial spray [11,24]. As such, ES has also been shown not to denature DNA during encapsulation [25]. Finally, when ES is used with multi-axial needles (Fig. 1) to develop immiscible layers of polymer, it can create core-shell or multilayer particles (Fig. 3). This can facilitate an additional controlled release feature of the particle, further dictating the kinetic release rates of the encapsulates [13]. These aforementioned features of ES make it a very advantageous particle generation method for a wide range of uses.

ES has been used for a vast variety of applications including material coatings [27], solar cells [28], tissue engineering [29], microfluidics [30], microelectromechanical systems (MEMs) [31], and drug delivery [13]. Since its first application in or around the mid-2000s for drug encapsulation [32], studies are beginning to move from developing the technique to applying it to relevant *in vitro* and *in vivo* systems. Several reviews exist regarding configurations and optimization of ES parameters, with most focusing on development of

the particle and/or *in vitro* release of cargo [1,2,13,29,33–36]. This review focuses on the reports of these particles being applied to cells and/or animal models and reports on the outcomes of these studies as they relate to advancements in the field of drug delivery, vaccine delivery, and tissue engineering.

2. Matrices used in electrospray

A variety of polymers have been applied to ES systems (Table 1), and this illustrates the broad variety of conditions that can be used to spray and form particles. When choosing a polymer there are several desirable physiochemical properties such as electrical conductivity, viscosity, and solubility that can be finely tuned to get the desired Taylor cone stability or particle size. Furthermore, if multi-axial ES is used, the miscibility of the solvents and polymers used will dictate whether core-shell or mixed phase particles are formed. There are several types of polymers reported here that are used in cell and animal models. These include polyesters, stimuli responsive polymers, natural polymers, and other non-degradable polymers.

2.1. Polyesters

The most used polymers for ES are by far poly(lactic-*co*-glycolic acid) (PLGA) and poly(lactic acid) (PLA). These are both polyesters, along with another commonly used polymer, polycaprolactone (*PCL*) and poly(glycolic acid) (PGA). Polyesters are biodegradable *via* hydrolyzable ester bonds. The ratio of glycolic acid and lactic acid in PLGA can be changed to somewhat alter the degradation rate, but generally 50:50 or 75:25 (PLA:PGA) polymers are used, with degradation rates on the order of months. With PLGA, the hydrolytic by-products are lactic acid and glycolic acid, with PCL yielding caproic acid. These acidic by-products have been shown to result in low pH locally [37], and in a particle form, PLGA has been shown to have pH ~3 inside particles [38,39]. Despite this, PLGA/PLA is a constituent of over a dozen FDA approved therapies, and because it has a valid drug master file, it is a common go-to polymer for drug delivery applications. Similarly, PCL has been approved in drug delivery and other devices.

2.2. Stimuli responsive

In this review, two primary stimuli are used to trigger the breakdown of ES particles: light and pH. Stimuli responsive materials can allow for release of encapsulate at a desired location or cell in the body, which can mitigate off-site toxicity as well as optimize therapy delivery. Carling et al. [41] formed a new light sensitive polymer called 2-(40-*N*-dimethylamino-4-nitro-[1,10-biphenyl]-3-yl)butane-1,4-diyl dicarbonyl for stimuli responsive delivery. As designed, the polymer degrades rapidly when exposed to visible light (λ_{ex} = 400–500 nm). This polymer was developed to degrade when visible light was focused at an intensity of ~0.21 W/cm^2 in the area of the delivered particles.

Acetalated dextran (Ac-DEX) has been used extensively by our lab and a few others for vaccine and drug delivery, including formulation *via* ES [3]. Ac-DEX is formed from dextran, an FDA approved polymer which is used as a plasma expander. The polymer is acid-labile and degrades more rapidly at lower pH, as observed intracellularly, near

inflammation, or in tumors. The by-products of Ac-DEX degradation are primarily dextran, as well as exceedingly low levels of acetone and a short chain alcohol (ethanol or methanol) [42], well below what is produced naturally in the body or would be toxic to even pregnant women [43,44]. A unique feature of Ac-DEX is its finely tunable degradation rate (from hours to months) [81] that can be adjusted with reaction time and dextran molecular weight [42,46]. Additionally, early studies with the material indicate that Ac-DEX stabilizes proteins outside the cold-chain [47]. Ac-DEX has yet to be in any FDA approved products, but has illustrated little to no toxicity in animal models [3,48].

Eudragits are another class of pH responsive polymers. They are a *co*-polymer comprised of methacrylic acid - methyl methacrylate, typically used for oral (PO) delivery [49]. They are non-degradable, nonabsorbable, and non-toxic polymers. The L series polymers are anionic and dissolve around pH > 6 for enteric coating and delivery to the small intestine. Eudragit RL series polymers have quaternary ammonium groups and although they are water insoluble, they are often applied for film coating because they afford sustained release *via* polymer swelling in aqueous systems.

2.3. Natural polymers

Besides polyesters, natural polymers are the most commonly used type of polymers applied in ES. Natural polymers can sometimes have distinct characteristics and easy and inexpensive sourcing compared to synthetic polymers, but they can also have known allergic responses that can limit their use.

Alginate is a natural anionic polymer derived from brown algae [50]. It can be easily cross-linked in the presence of divalent cations such as Ca^{2+}. Unless modified to become degradable, alginate is generally non-degradable in mammals. Particles made from alginate can be easily fabricated by dripping a solution of the polymer into a Ca^{2+} aqueous solution. Because of the ease of fabrication, alginate is used commercially in food (*e.g.* gummies, boba tea) as well as for oral delivery capsules.

Cellulose derivatives are used for ES and are usually modified to make them more soluble in organic solvents. Ethyl (hydroxyethyl) cellulose (EHEC) is a cellulose based polymer where ethyl and hydroxyethyl groups are linked to anhydroglucose units by ether linkages. Carboxymethylcellulose (CMC) has carboxymethyl on many of the hydroxyl groups of the glucopyranose monomers [51]. Both polymers degrade as cellulose degrades. They are both also used commercially as a thickening agent and to deliver drugs orally.

Gliadin is a wheat storage protein [58]. It is the water-soluble portion of gluten, which can limit its use to individuals who are not gluten sensitive. To that point, gliadin is the main immunogen of Celiac disease. Gliadin is often a contaminant detected in pharmaceutical preparations and is typically purified for formulation use.

Gelatin is a water soluble, denatured version of collagen. It is used as a gelling agent in many things including food and pharmaceuticals. As a protein, it is degradable in the body. It is often used to enhance cell adhesion for electrospinning [54] since it possesses binding groups for integrin binding of most cells.

Fibroin is an insoluble protein that is contained in spider silk [60]. Its primary structure consists of repeat sequences of amino acids $(GlySer\text{-}Gly\text{-}Ala\text{-}Gly\text{-}Ala)_n$, to form anti-parallel beta sheets. These consecutive beta-sheets give the material a high stiffness and strength. Some bacteria are able to degrade fibroin, while mammalian species cannot.

Maize arabinoxylans are the main non-cellulose polysaccharides in corn. They can form gels in aqueous environments. Bran is the primary by-product of corn milling and mostly comprised of cellulose. Corn wax is the solid that is formed from the chilling of corn oil during the refining process and can be used for soap stock [61]. As polysaccharides, the structures are likely degradable, although this is not well understood.

Chitosan is a polysaccharide that can be isolated from various shellfish such as shrimp and crab. Since it is isolated from shellfish, there is concern that it could cause anaphylaxis in those who have shellfish allergies. A unique property of chitosan is that it is mucoadhesive and is commonly used for PO delivery, as it will attach to the mucous layer of the gastrointestinal tract. It is degradable and considered non-toxic but has not been FDA approved for use as a drug delivery polymer.

Yams are a very common plant across the globe. The starches from a yam have been shown to be viscous and stable in acidic conditions. They can be substituted for modified starches in processed foods and have been applied in the food industry. Their application in pharmaceutical has not been well reported [65].

2.4. Cationic polymers and lipids

Polyethylenimine (*PEI*) is a polymer comprised of repeat amine groups. It can be linear or branched. Abundant amines make the polymer highly cationic. When mixed with DNA or other negatively charged species, it can form polyplexes where the oppositely charged species intermix. At high levels PEI can be cytotoxic because the cations can complex to the cell's DNA [69].

1,2-dioleoyl-3-trimethylammonium-propane (DOTAP) is a cationic phospholipid. It can be used in liposomes and other lipid complexes to provide a positive charge. Additionally, it can serve as an amphiphilic lipid to reduce surface tension and stabilize the surface of the particle.

2.5. Other non-degradable polymers

Ecoflex® is a rubbery material that is commonly used to make masks and prosthetics. It is approved for dermal contact but has not been approved for use in the body. The polymer is a non-degradable platinum-catalyzed silicone. Its ability to stretch and deform can afford it unique properties when formulated into particles.

Polyethylene glycol (*PEG*) is one of the most commonly used polymers for biomedical applications since it is highly thermodynamically favorable for it to interact with water. Due to this, it has anti-fouling properties that resist protein and cell adhesion, leading to reduced clearance by the reticuloendothelial system. This leads to long circulation times when therapeutics that are PEGylated (covalently bound to PEG) are given intravenously.

Moreover, steric protection of protein therapeutics can occur, leading to reduced absorption or degradation of these therapies. The first PEGylated therapy was PEG covalently attached to interferon, and since then there have been more than a dozen PEGylated therapies including conjugates to proteins, peptides, aptamers, and even small molecules. Liposomal doxorubicin (Doxil®) is a PEGylated liposome and the most commercially applied liposomal therapy. PEG is not degradable, and often is used at molecular weights which will clear the kidney (< 40 kDa) because it will, over time, disassociate from the conjugate. There are reports of immune responses to PEG, which can complicate its use in humans [76].

Polyvinyl alcohol (PVA) is a common additive in polyester emulsions. It is a non-degradable material at realistic timescales in the body and is also water soluble. It is used as a thickening agent in drug formulations like eye drops. The addition of PVA to emulsions or ES can result in a more viscous solution, which could result in a more stable emulsion or Taylor cone.

3. Applications

3.1. Drug, protein, cell and gene delivery

3.2. Cancer drug delivery

The most common application of ES particles is for delivery of chemotherapeutics to treat cancer (Table 2). Since most ES particles are too large to exhibit the enhanced permeability and retention (EPR) effect [95], and intravenously (IV) injected particles primarily accumulate in the liver and spleen, direct injection into the tumor or peritumoral injection would be preferred. Intratumoral (IT) injections can be clinically relevant [96] for melanoma and other accessible cancers, and as cancer imaging techniques improve [97], this method of administration becomes more and more of an option for treatments.

3.2.1. Glioma treatment—Cancers affecting glial cells in the brain, known as gliomas, are the most studied cancers for application of ES particles (Table 2). Since surgical resection is the standard of care for brain cancer [98], interstitial therapy, where therapeutic agents are administered to the tumor resection cavity, can be easily applied. The FDA approved Carmustineloaded Gliadel® wafers are based on this practice. This therapy has significant room for improvement since Carmustine has low tumoricidal activity and is rapidly cleared from the brain upon release from the polymer wafer [99–101]. In 2005, Ding et al. [82] first reported the application of PCL particles encapsulating taxol, prepared *via* monoaxial ES, for the treatment of rat C6 Glioma cells *in vitro*. They noted that cellular uptake of particles was approximately 60% after 2 h of incubation and varied slightly with different processing parameters, including where the particles were collected during post spray processing (*e.g.* filter, pre-filter). Xie et al. [83] then expanded on this work in the following year by preparing paclitaxel-loaded PLGA ES particles 200 nm to 10 μm in size. These particles illustrated an increase in the ratio of G_2/M (interphase to mitosis) in C6 cells, mostly as the dose of paclitaxel increased in the particles. Moreover, C6 viability decreased with drug loaded particle treatment in a time but not dose dependent manner, when given *in vitro*. Later, Ranganath et al. [85] (Fig. 4) took ES paclitaxel

PLGA microparticles suspended in a sodium alginate solution and electrosprayed them a second time directly into a $CaCl_2$ solution. They then encapsulated the PLGA microparticles into alginate hydrogel beads approximately 1.6 mm in size. When C6 glioma cells were cultured with the microparticle-hydrogel composite, greater apoptosis was observed for the encapsulated group at 6 days, compared to the soluble drug control; however, it was not significant *versus* the soluble drug at 2 and 4 days. The 50% lethal dose (LD_{50}) of the formulation was significantly changed when the gelation time of the alginate beads (time in the $CaCl_2$ solution) was altered, with increased gelation time leading to reduced cytotoxicity. Using another glioma cell line, GL261, Hayashi et al. [86] report cytotoxicity of red blood cell-like ES EHEC particles on the order of 1 to 10 μm in size, encapsulating superparamagnetic magnetite nanoparticles. In a very limited study, the cytotoxicity of the composite microparticles was reported to be the same as the control. In another study, Nie et al. [87] used co-axial ES to co-encapsulate paclitaxel and suramin in PLGA particles approximately 10 to 20 μm in size. When evaluating the co-therapy particles against a human glioma cell line, U87, they note an ~20% reduction in proliferation and viability after 3 days. Also, higher levels of apoptosis were observed with the co-therapy particles compared to free compound, but only after 6 days. Ramachandran et al. [91] also used U87 cells and treated them with PLGA ES particles encapsulating the photo-labile porphyrin 5,10,15, 20-tetrakis(*meso*-hydroxyphenyl)porphyrin (mTHPP) coated in albumin with dasatinib. When applied to U87 cells, a dose and time dependence for uptake was reported. When laser assisted activation of mTHPP was used, they noted an increase in reactive oxygen species (ROS) production by the glioma cells. Additionally, they noted inhibition of cell migration as a result of dasatinib. With these studies, they illustrated activity on U87 cells of both porphyrin and the tyrosine kinase inhibitor. In general, these studies illustrate that ES particles can release chemotherapeutics to lyse glioma cells in culture, particularly at longer time points, indicative of a controlled release system.

Although promising *in vitro* studies have been reported for the treatment of glioma cells with ES particles, evaluation in an animal model can advance pre-clinical studies toward the eventual translation of these therapies. Naraharisetti et al. [84] encapsulated both paclitaxel and etanidazole into 15 μm particles using monoaxial ES. When these particles were given in peritumoral implants for the treatment of a subcutaneous C6 tumor in BALB/c nude mice, cell death was observed histologically at the tumor edge. Decreased tumor volume was observed in the co-therapy particle group compared to soluble therapies. In comparison to other particle types, ES and spray dried particles displayed the same tumor inhibition with a four times lower dose of paclitaxel compared to disc shaped particles. Using the same animal model, Ranganath et al. [85] (Fig. 4) expand on their *in vitro* studies to show that after 21 days, tumor volume was reduced by paclitaxel loaded PLGA particles prepared *via* monoaxial ES, compared to untreated and soluble drug controls. They performed an IT incision to deliver 2 mg of particles and used valid sham controls for this method. Nie et al. [87] used a similar model with U87 cells in place of C6 cells to continue their *in vitro* work. Co-encapsulating paclitaxel and suramin, they found that localization of one drug *versus* the other in the core or shell of the particles did not result in significant differences in GBM growth. Additionally, statistical differences were not noted between individually delivered drugs and co-encapsulated compounds for tumor growth inhibition. However,

histology showed fewer tumor cells and reduced proliferation with co-encapsulated particles. These studies illustrate the ability of ES particles to treat glioma cancer burdens *in vivo*, and significantly reduce the tumor burden in comparison to soluble drug controls. Moreover, ES affords the co-encapsulation of multiple drug therapies for enhanced treatment of glioma.

3.2.2. Other cancers—Several other studies have reported ES particles encapsulating chemotherapeutics for the treatment of other cancers such as breast, skin, lung, liver, or ovarian. Two studies have evaluated ES particles for the treatment of breast cancer. Using doxorubicin encapsulated in 300–1800 nm co-axial electrosprayed silk and PVA particles, Cao et al. [79] observed a dose and time response in cytotoxicity when MDA-MB-231 breast cancer cells were cultured with the particles. The cytotoxicity observed upon treatment with the doxorubicin particles was greater than treatment with soluble drug at the same concentration. Additionally, apoptosis increased in a dose and time responsive fashion with the particles and further increased when ultrasound was introduced to the culture. Applying MCF7 breast cancer cells *in vitro*, Gulfam et al. [88] used monoaxial ES to encapsulate cyclophosphamide into 200–400 nm gliadin and gelatin-gliadin nanoparticles. When cells were cultured with the particles, B-cell lymphoma 2 (BCL-2), a regulator of cell death, was downregulated in cells treated with soluble drug or particle-delivered drug. Moreover, they report there were no significant differences in BrdU incorporation between the soluble and encapsulated drug after 24 h, indicating no significant differences in cell proliferation. Looking at melanoma, Cao et al. [89] loaded combretastatin A4 and doxorubicin into composite PLGA, PCL, and PVP particles using a co-axial ES system. They evaluated the drug activity *in vitro* against B16-F10 melanoma cells and human umbilical vein endothelial cells (*HUVECs*). They noted that the co-encapsulated particles induced apoptosis in both cell types. Applying silk fibroin particles approximately 60 nm in size and encapsulating cisplatin, Qu et al. [90] evaluated lung cancer cells. They observed an increase in platinum uptake in lung cancer A549 cells over non-cancer L929 cells when cultured with particles containing the platinum-based cisplatin. The particles were able to induce cytotoxicity at an increased rate *versus* soluble drug or empty carrier. Yin et al. [92] used ES to encapsulate gambogic acid into PLA microparticles to evaluate *in vivo* for the treatment of a hepatocellular carcinoma using an H22 cell orthotopic model. In a distribution study with intravenous administration, they found that particles smaller than 185 nm accumulated the most in the liver, whereas those around 350 nm in size collected most extensively in the spleen and those approximately 7 μm in size had the highest accumulation in the lungs. This distribution correlated with the ratio of gambogic acid in a specific tissue to the ratio in all the tissues evaluated (*i.e.*, heart, liver, spleen, lung, kidney). Survival time of mice inoculated with liver cancer was improved with the drug loaded particle group over the soluble drug group. Zhang et al. [93] used co-axial ES to encapsulate both paclitaxel and etoposide into core-shell PLGA particles. They report that the encapsulated drugs increased cytotoxicity when applied to osteosarcoma cells, in comparison to free drug alone. Varshosaz et al. [75] (Fig. 5) evaluated ovarian cancer SKOV-3 cells both *in vitro* and *in vivo* using monoaxial ES particles comprised of Ecoflex® and PEG to encapsulate docetaxel. They noted that *in vitro*, particles significantly decreased cell viability *versus* free drug at the same concentration. This correlated with particle uptake, in that rhodamine B labeled particles were taken up at an increased rate

compared to free dye, as measured with flow cytometry. When applied *in vivo* to a B6 nude mouse model with subcutaneously introduced SKOV-3 ovarian cancer cells, the tumor size was significantly reduced in the particle treated group compared to the saline or Taxotere control without significant difference in body weights between groups. These results in an *in vivo* ovarian cancer model indicate that chemotherapeutic-loaded ES particles can reduce *in vivo* tumor burden, advancing the promising application of ES particles for delivery of chemotherapeutics. Watkins-Schulz et al. [94] used the stimulator of interferon genes (STING) agonist, cyclic guanosine monophosphate–adenosine monophosphate (cGAMP), as immunotherapy for cancer and illustrated innate immune signaling activity in bone-marrow derived dendritic cells (BMDCs). Production of inflammatory cytokines interferon-beta (IFN-β), tumor necrosis factor (TNF), and interlukin-6 (IL-6) all were significantly greater when cGAMP was encapsulated in electrosprayed Ac-DEX microparticles than when given in soluble form. cGAMP microparticles were injected *via* various routes in a subcutaneous B16F10 mouse model of melanoma, with IT injection illustrating the greatest reduction in tumor burden. Using this route of administration, tumor burden was significantly reduced in both melanoma and breast cancer (e077), in a manner that was dependent on natural killer (NK) and CD8+ T cells. When a STING knock-out mouse (6(Cg)-Tmem173tm1.2Camb/J (Tmem173−/−)) was used, cancer growth was not significantly changed, indicating that STING is required for cGAMP microparticle efficacy. All of these studies collectively expand on the application of ES particles to deliver chemotherapeutics to impact the growth and viability of several cancer types.

3.3. Antimicrobial delivery

The controlled release of antimicrobials can lead to reduced treatment frequency, which can result in reduced emergence of drug resistance and better treatment of biofilms [104]. To this end, several anti-microbial compounds have been encapsulated in ES particles and have demonstrated efficacy both *in vitro* and *in vivo* (Table 3). Duong et al. [18] loaded the toll-like receptor 7/8 agonist resiquimod into Ac-DEX microparticles using monoaxial ES. Particles were made with different drug loadings. When cultured with RAW macrophages *in vitro*, less resiquimod was needed for similar cytokine production when the drug was encapsulated in Ac-DEX particles, but this result was only observed when particles had a higher drug loading. Viability and proliferation of cells was equivalent for all particle groups except at high concentrations of particle and with the lower drug loaded particles. Using an *in vivo* visceral *Leishmania donovani* model of infection, mice were treated with either blank or drug-loaded microparticles *via* IV injection on day 14, post infection. Parasite burden in the bone marrow of infected mice at day 28 was significantly reduced by treatment with resiquimod loaded microparticles compared to treatment with empty microparticles. Parasite burden in the liver and spleen were numerically reduced but were only significantly lower than the PBS control in the liver. In another study evaluating the toxicity of tetracycline hydrochloride encapsulated in monoaxial CMC alginate particles, Lai et al. [102] applied particles 500 nm in size to 3T3 fibroblasts and human embryonic kidney (HEK293) cells. They illustrated that cytotoxicity remained near 100% at a concentration up to 200 μg/mL at 5 and 24 h. Mai et al. [103] (Fig. 6) encapsulated curcumin in PLA monoaxial ES particles, forming 1–20 μm particles. They evaluated antibacterial efficacy in *Escherichia coli* (*E. coli*) and *Staphylococcus aureus* (*S. aureus*) using a disc approach

on bacterial lawns on agar. They illustrated that discs comprised of the antibiotic loaded particles limited the growth of either bacteria. They also noted low levels of hemolysis and cytotoxicity in rat adrenal medulla (PC12) and human embryonic kidney (293 T) cells, and these low levels were observed to have a dose response. When human dermal fibroblasts were grown on a layer of particles, a growth rate similar to tissue culture plastic control was observed at 1, 3, and 5 days. These studies are a start to applying an ES platform to an area of increasing interest, antimicrobials. As drug resistance to conventional antimicrobials increases, ES particles could be a valid controlled release system that should be explored to decrease dosing frequency.

3.4. Oral delivery

Oral delivery of therapeutics is always challenging due to significant barriers which can include extreme pH levels, intermittent fluid flow, high amounts of metabolizing enzymes, and a discontinuous mucosal layer across the entire gastrointestinal tract [109]. Platforms that can effectively deliver biologics and small molecules which do not obey Lipinski's rules through the oral route are desired, as current approaches result in very poor bioavailability. Several ES particles have been applied for oral delivery (Table 4). For example, Hao et al. [105] encapsulated proton pump inhibitor omeprazole into Eudragit L 100–55 monoaxial ES particles. At the highest drug to polymer ratio (0.8), cytotoxicity in Caco-2 intestinal epithelial cells was significantly lower at 24 h compared to untreated controls. Later at 36 and 48 h, particles with lower drug to polymer ratios (0.4 and 0.6) also had reduced cytotoxicity compared to controls. In a separate work, Hao et al. [106] evaluated the cytotoxicity of PLGA particles encapsulating the anti-ulcer medication metronidazole with GES-1 (gastric epithelial) cells. These formulations were non-toxic to cells up to 800 μg/mL at 24 h. Cytotoxicity decreased very slightly with 2–4% *w*/w loaded particles at the 36 and 48 h time points. In a third study by Hao et al. [107], aspirin was encapsulated *via* co-axial ES into Eudragit L 100–55 and Eudragit RS particles. Cytotoxicity of Caco-2 cells when incubated with aspirin-loaded particles was significantly reduced after 24 h at a particle concentration of 100 μg/mL and greater. For all evaluated drug concentrations, cytotoxicity was significantly reduced at 36 and 48 h. A dose and time dependent response was observed with cytotoxicity measurements, reporting levels as low as 65% viability for 800 μg/mL at 48 h. When Caco-2 cells were imaged for uptake by epifluorescence, there was notable uptake at 1 and 2 h. In another application of ES particles for oral delivery, Paz-Samaniego et al. [108] (Fig. 7) used corn-based bran and wax arabinoxylans to encapsulate bacteria and insulin *via* tetra-axial ES. Using the SIMulator Gastro-Intestinal (Simgi®)—a computer-controlled model of a human GI tract that consists of five successive reactors, simulating the stomach, small intestine, and three parts of the large intestine—they report that 24% of insulin was released before the colon compartment, with the remainder released in the colon. Bacteria deposition was noted in the colon compartment, but earlier deposition was not discussed. Overall, oral delivery of small molecule drugs, proteins, or cells has been reported with ES particles, illustrating the promise of this technique in developing platforms for oral drug delivery.

3.5. Gene delivery

For gene delivery, PEI has been used in two ES applications, one that formed PEI-DNA polyplexes during spraying and another that induced transfection as part of the process. Zeles-Hahn et al. [70] sprayed PEI and the cationic lipid DOTAP with plasmid DNA encoding luciferase. They reported a significant increase in cytotoxicity when 1:10 DNA to PEI polyplexes were applied to human derived tracheal epithelial cells, but such an increase was not observed with a 1:4 polyplex. Both lactate dehydrogenase (LDH) release and interleukin-8 (IL-8) were measured, demonstrating both cytotoxicity and cytokine production increase in < 10 h. Lee et al. [71] electrosprayed PEI with plasmid encoding green fluorescent protein (GFP) and 3T3 fibroblasts, all in a single spray, as a form of aerosol electroporation. They concluded that transfection increased when different media was sprayed and when a range of voltages were applied to the spray needle. The viability of the cells decreased with increasing electrical potential difference between the spray needle and substrate. Together, these studies demonstrate promise for the future applications of ES in gene transfection (Table 5).

3.6. Treatment of inflammation and oxidative stress

ES particles have been used for a variety of other drug delivery applications including treatment of inflammation and oxidative stress. In a study using a photosensitive polymer, 2-(40-*N*-dimethylamino-4-nitro-[1,10-biphenyl]-3-yl)butane-1,4-diyl dicarbonyl, Carling et al. [41] (Fig. 8) evaluated the inhibition of inflammation by encapsulating dexamethasone using monoaxial ES to form particles approximately 1 μm in size. Using a carrageenan-induced hind paw inflammation model and treating with particles, they report that application of light to rapidly degrade the particles resulted in significantly reduced footpad thickness, indicating reduced inflammation, compared to dexamethasone alone or drug in the particle without light exposure. Stubelius et al. [110] used ES to encapsulate dexamethasone in Ac-DEX particles and evaluated them in cells, a dermal air pouch model, and an animal model for gout. They report reduced IL-1β levels in mouse bone marrow derived macrophages and CXCL1 levels in epithelial cells when cells were stimulated with lipopolysaccharide (LPS) and monosodium urate (MSU) crystals and then incubated with particles. Upon treatment with dexamethasone-loaded Ac-DEX particles, pro-inflammatory cytokine levels were significantly reduced compared to untreated PBS controls but not compared to dexamethasone-loaded PLGA particles or the free drug. Prophylactic treatment of an MSU mouse model of gout lead to significantly reduced tissue infiltration of the MSU crystals compared to untreated control, free dexamethasone, and PLGA-encapsulated dexamethasone. Prophylactic treatment was also evaluated in a skin air-pouch model to determine the inflammatory response of the formulation. Similar to the gout model, the Ac-DEX-encapsulated dexamethasone group significantly outperformed the other groups in the reduction of pro-inflammatory cytokines and immune cell infiltrates.

Looking at oxidative stress, Xing et al. [111] used a tri-axial ES to make porous PCL particles loaded with antioxidant Ganoderma lucidum polysaccharide (GLP) in a solid core-porous shell structure intended for pulmonary delivery. Though the particles seem large with an average size of 13.37 μm, the theoretical mass mean aerodynamic diameter ($MMAD_t$) was estimated to be 4.66 μm. This $MMAD_t$ paired with the particle porosity made

the formulation promising for aerosolization and lung delivery [111]. These particles were administered to an H_2O_2-induced oxidative stress *in vitro* model with MRC-5 human lung fibroblasts. After 48 h treatment with particles, reactive oxygen species (ROS) staining indicated a reduction in ROS, and 3-(4,5-dimethylthiazol-2-yl)-2,5-diphenyltetrazolium bromide (MTT) indicated an increase in cell proliferation and viability. Furthermore, Sudan Red G loaded particles were delivered *via* a dry powder insufflator, *in vivo* to determine biodistribution upon inhalation by pathogen-free KunMing mice. Fluorescent intensity measured *in vivo* demonstrated delivery to the lung tissue and a retention time > 48 h. Overall, these applications of ES for stimulus-sensitive delivery and pulmonary delivery demonstrate the promise of the ES method for control of oxidative stress (Table 6).

3.7. Vaccine delivery

The application of ES for production of particulate vaccines takes advantage of the reduced denaturation of encapsulated proteins and peptides compared to other formulation methods, such as emulsion. Reduced denaturation is desirable for subunit vaccines that use proteins as antigens. In the evaluation of vaccines, only innate signaling can be evaluated *in vitro* with leukocytes, so mouse or higher species models must be used to fully elucidate the protection afforded by vaccines. Suksamran et al. [65] report development of an orally delivered vaccine comprised of alginate or yam starch encapsulating the model protein ovalbumin and coated with a cationically modified chitosan through electrostatic interactions. They noted that when the particles were applied to Caco-2 cells, cell viability was essentially 100% in particle concentrations up to about 1 mg/mL, and cytotoxicity increased to near 50% at > 10 mg/mL of particles. They then evaluated adhesion of the particles in an *ex vivo* porcine intestine model. Adhesion to the porcine intestine after 30 min was significantly greater for cation-coated particles relative to uncoated particles, and a fairly constant percent adhesion was observed in all groups out to the last time point at 2.5 h. Particles were then evaluated in BALB/c mice for antibody titer generation following oral vaccination on day zero with another orally administered booster dose on day fourteen. Significantly greater total IgG and IgA titers were observed from mice vaccinated with chitosancoated, OVA-loaded alginate yam core particles compared to individual polymer formulations and formulations without yam protein. Doavi et al. [112] used a monoaxial electrospray strategy to encapsulate a synthetic *E. coli* antigen, rEIT, into chitosan or trimethylated chitosan (TMC) particles. They administered the antigen encapsulated in either vehicle intranasally to BALB/c mice, with boosts on days 28 and 42 following initial vaccination. Comparable levels of anti-rEIT IgG in serum was observed when immunizing with ES formulations or a positive control consisting of rEIT injected intraperitoneally with Freud's adjuvant. In addition, they saw increased anti-rEIT IgA titers in serum, fecal, and eyewash fluids compared to both the soluble controls and the intraperitoneal positive control. Subsequently, they observed significantly reduced adhesion of *E. coli* O157:H7 to cultured Caco-2 monolayers in the presence of sera from the intranasally immunized mice relative to unimmunized mice. Bacterial shedding from the intestines was also significantly reduced compared to soluble controls in both groups immunized with ES particles. Gallovic et al. [11] generated an anthrax vaccine using Ac-DEX to encapsulate recombinant protective antigen (rPA) and resiquimod either together or in separate particles using co-axial ES (Fig. 9). Vaccinating on day 0 and 21 subcutaneously

in BALB/c mice, we showed that vaccination with ES particles significantly increased the amount of total IgG, IgG2a isotype, and neutralizing antibodies compared to particles made through emulsion. Also, ES particles protected significantly better after a lethal aerosol anthrax challenge. Moreover, we showed that ES particles protected better than rPA with alum or FDA approved Biothrax. In a lethal challenge, we reported that, surprisingly, co-encapsulated particles (rPA and resiquimod) provided significantly reduced protection than when adjuvant and antigen were separately delivered, despite having similar total IgG titers. Junkins et al. [48] also applied Ac-DEX using a co-axial ES system to develop an influenza vaccine using hemagglutinin (HA) and STING agonist cGAMP. In this study, cGAMP was encapsulated in Ac-DEX particles and HA was delivered in soluble form. When culturing BMDCs isolated from C57Bl/6 mice with cGAMP particles, ES Ac-DEX particles had significantly greater induction of IFN-γ and IL-6 than unloaded particles, ES PLGA particles, emulsion Ac-DEX particles, liposomes, or transfection agent co-administered with cGAMP. We also reported that no significant differences in IFN-γ secretion were observed when treating BMDCs with cGAMP particles before or after sterilization with gamma-radiation. Vaccinating mice *via* intramuscular (IM) injection on day 0 and 21, we reported there was greater total IgG, IgG2a isotype, soluble cytokines, and cells producing IFN-γ and IL-2 after HA re-stimulation compared to controls. These differences became significantly greater as the concentration of cGAMP decreased. Additionally, mouse toxicity studies were performed, and across six different parameters, cGAMP-loaded particles at the highest loading did not illustrate any signs of toxicity. Furtmann et al. [80] used monoaxial ES to encapsulate Cytomegalovirus (CMV) pp65 IE-1 peptide. They then administered the particles to peripheral blood mononuclear cells (PBMCs). They noted that cytotoxicity was not decreased with increasing concentration of peptide loaded particles, and particles did not significantly change cytotoxicity. Additionally, monocytes primarily took up the particles in contrast to B cells, T cells, and NK cells, which is logical for 200 nm sized particles as they can only effectively be engulfed by phagocytic cells [113]. TNF-α and IFN-γ positive T cells were near equal with those treated with soluble peptide after antigen re-stimulation. Although, they reported significantly increased T cell proliferation with particle treated PMBCs compared to those treated with soluble peptide. Increased peptide tetramer staining over soluble and blank particle control was also reported after particle treatment. Chen et al. [45] used Ac-DEX and encapsulated ovalbumin and murabutide, separately, using co-axial ES to explore the effect of particle degradation on vaccine responses. When particles encapsulating the NOD-2 agonist murabutide were applied to JAWSII dendritic cells, we found that significantly higher production of cytokines over soluble, blank, or media control was observed when the adjuvant was delivered with ES particles. Furthermore, cell viability was near 100% for up to 400 ng/mL of murabutide. To understand the effects of degradation individually on adjuvant (murabutide) and antigen (ovalbumin), particles encapsulating these compounds were co-delivered with soluble ovalbumin or monophosphoryl lipid A (MPL), respectively. After IM vaccination on day 0 and 21 with particles of three different Ac-DEX degradation rates for both adjuvant and antigen delivery, total sera IgG and isotypes were shown to be uniquely dependent on the degradation rate of Ac-DEX polymer. Moreover, cellular responses were influenced by degradation, in a manner unique in some cases from what was observed with humoral responses. These studies support the idea that encapsulation with ES is desirable for protein delivery, as a denatured protein would not

elicit a strong humoral or protective response for many of these evaluated systems. As the application of ES for vaccine development grows, other benefits like scalability and dry powder formulation will likely also contribute to the success of this platform (Table 7).

3.8. Drug release for tissue engineering

The range of tissue engineering applications of ES particles is vast and includes drug releasing particles as well as using blank particles to create microstructures, such as pillars of particles or particle laden nanofibers [29]. These surfaces create structure for new tissue growth, differentiation and repair. To accomplish this, even a variety of matrix material, outside the realm of polymers have been used. For example, Link et al. [124] report the electrospray of decellularized extracellular matrix to form nanoparticles and promote lung repair. Several reviews discuss the application of electrospray particles strictly for tissue engineering [29,125,126]. In noting the studies that generate drug eluting particles applied *in vitro* or *in vivo*, two primary applications are found: stem cell differentiation and encapsulation or bone tissue repair Table 8.

ES has been used to generate particle laden scaffolds or scaffold components for stem cell differentiation, and it is also used to encapsulate cells for tissue engineering applications. Wang et al. [114] (Fig. 10) fabricated PLGA and gelatin particles to encapsulate insulin-like growth factor (IGF). These particles were then sprayed on to polyurethane urea scaffolds that were simultaneously being electrospun. When mesenchymal stem cells (MSCs) were seeded on the particle laden scaffolds, the IGF released from lower molecular weight PLGA lead to increased proliferation of rat aortic smooth muscle cells (SMCs). MSC viability on the scaffolds was the greatest with the low molecular weight particles incorporated in the scaffold; however, those grown on high molecular weight particle scaffolds exhibited similar viability. Under hypoxic conditions, the MSCs had significantly lower viability when grown on a scaffold without IGF incorporated in the particles compared to being grown on a scaffold with IGF loaded in the ES particles. In another approach, focusing on the encapsulation of cells, Zhao et al. [118] electrosprayed R1 Embryonic stem cells in either alginate or carboxymethyl cellulose (CMC) to form either gel (alginate) or liquid CMC containing particles. They showed that the gel core had decreased pluripotency markers and increased differentiation markers for cardiac cells, whereas the liquid core particles displayed the opposite trends. However, in culture, the cells in the liquid core displayed significantly more beating foci, indicative of cardiomyocyte activity. Additionally, the gel core particles still displayed increased foci compared to tissue culture control. Zamani et al. [119] encapsulated Stromal derived factor-1α (SDF-1α) with and without bovine serum albumin (BSA) in ES PLGA co-axial particles. When the particles were applied to MSCs *in vitro*, a significant increase in number of migrating cells was observed in response to particles containing both BSA and SDF-1α compared to particles without BSA and other controls. Moreover, MSCs proliferated at an increased rate when cultured with extract released from the BSA stabilized particles. Gandhimathi et al. [120] used monoaxial ES to encapsulate ascorbic acid and dexamethasone into PCL and silk fibroin, forming particles 0.72 to 4 μm in size. When the co-therapy particles were incubated with human adipose derived stem cells (ADSC), cells grown on the particles had increased growth across all timepoints compared to tissue culture controls, individual and combined polymer

blanks, and polymers with ascorbic acid. Quantification of alkaline phosphatase (ALP) activity showed that osteogenic differentiation was highest in the co-therapy particulate group, as well as the particle group without dexamethasone. This mirrored the highest mineral deposition observed. Evaluating the encapsulation of cells *via* ES, Esfahani et al. [122] encapsulated 3T3 fibroblasts into rigid PLGA microparticles using co-axial ES. They illustrated encapsulation of GFPexpressing fibroblasts using flow cytometry and microscopy. In the same year, Chang et al. [123] loaded bone morphogenetic *protein-2* (BMP-2) into PLGA particles and then embedded them in a cryogel scaffold. The scaffold was placed under the head of a screw as it was implanted into the mandible of a rat. The bone to volume ratio around the screw increased for all groups, compared to PBS control, but the deposition of new bone was greatest for the particle-containing group. These studies indicate that systems with ES particles can influence stem cell differentiation into a variety of different tissues.

For bone tissue repair a variety of ES platforms have been evaluated. Chang et al. [115] have used PLA and PLGA and co-axial ES to encapsulate platelet-derived growth factor (PDGF) and simvastatin, used to stimulate osteoblastic activity [127]. Osteotomies (*i.e.* holes were drilled in the bone) were performed on Sprague-Dawley rats, where a section of bone was removed from the maxillae. Looking at osteotomy repair and bone regeneration, they showed that simvastatin-in-core and PDGF-in-shell particles had significantly greater percent of bone fill compared to controls, individual drug groups, or the PDGF-in-core and simvastatin-in-shell group. Significantly fewer inflammatory cells were observed in the co-delivered groups. However, tartrate-resistant acid phosphatase positive (TRAP+; a marker of osteoclasts) cells and apoptotic cells (except for the PDGF-in-core/simvastatin-in-shell particles) in all drug treatment groups were similar by day 14. They continued this work, using the same particle system and animal model, osteotomy repair in Sprague-Dawley rats [123]. They then report significantly greater osteogenesis in the osteotomy with core-shell PDGF and simvastatin particles at day 14, but by day 28 bone growth was similar in all drug groups, including individually delivered agents. TRAP+ cells significantly increased, compared to BSA core/shell control, after treatment with simvastatin-in-core with BSA-in-shell or simvastatin-in-core and PDGF-in-shell after 28 days. Nath et al. [116] used simvastatin alone in PLGA monoaxial ES particles. When these particles were cultured with MG-63 osteoblast cells the cytotoxicity of simvastatin loaded particles was reduced compared to PLGA alone, especially at higher drug loading. Expression of osteogenic factors, determined by PCR, significantly increased with simvastatin dose and time up to 14 days compared to the PLGA control for all recorded time points. Wang et al. [121] (Fig. 11) encapsulated vascular endothelial growth factor (VEGF) and *BMP-2* into 500 nm PLGA and PLA co-axial ES particles. Using microvascular epithelial cells (MECs) and the osteogenic differentiation of bone marrow stem cells (BMSCs) they showed that VEGF induces MEC proliferation and gene expression of ALP, and osteopontin (*OPN*) and BMP-2 were significantly increased with BMP-2 treatment after 14 days. Using a rat calvarial bone defect model, they showed that treatment with co-therapy particles lead to significant increases in bone volume at 2, 4, and 8 weeks compared to soluble agent, even co-delivered soluble agent. Additionally, CD-31 presence at 4 and 8 weeks was significantly greater compared to soluble controls, combination soluble controls, and blank particles, indicating

greater vascularization upon co-therapy particle treatment. Increased osteocalcin (OCN) for co-therapy particles *versus* other groups was illustrated *via* histology. The application of ES particles for bone tissue engineering has illustrated strong repair, bone growth, and expression of repair-associated factors. These promising results should encourage further exploration of the applications of ES therapies for bone growth and repair. ES is starting to emerge as a platform for tissue regeneration and these results are promising in the field of tissue regeneration and drug delivery.

4. State of the art and future perspectives

As demonstrated by the works highlighted here, ES technology is promising for various biomedical applications, including cancer treatment, vaccine development, oral drug delivery, and drug eluting tissue engineering platforms. ES also promises advantages over other particle fabrication techniques when it comes to manufacturing. Additionally, ES demonstrates improved encapsulation efficiency over other techniques. Despite these advantages, there is a need for improved methods to evaluate particle cytotoxicity in cell culture and for more rigorous animal models in the evaluation of ES drug-loaded particles.

With regard to manufacturing, the scalability and size of the ES system could advance its application in cell and animal models. The scalability of ES is a significant advantage of the platform. Although others have studied multi-plexing of ES systems where multiple spray nozzles operate in parallel [20,21], this has not been reported to be applied to *in vitro* and *in vivo* models. Comparison of multi-plexed *versus* single-head systems *in vivo* would advance the scalability potential of the platform. To display a bioequivalence of sorts between the two methods would lead to better acceptance of ES for the fabrication of particles en masse. In addition to scalability, a smaller size of particles would lead to a better embrace of ES particles by the biomedical community. A majority of the studies above report particles with diameters > 200 nm and into the micron range. To target non-phagocytic cells and for better intravenous delivery of particles, which would be especially helpful for the delivery of chemotherapeutic or theranostic agents in cancer treatment, sizes 100 nm or below are needed. Generation of particles in this size range and in a multi-plexed model would have significant impact on ES for biomedical applications.

In selection of cargos, a focus should be placed on molecules that need to be encapsulated for maximum efficacy. Also, molecules that have poor encapsulation with other methods —often due to partitioning into an aqueous continuous phase present during processing —increases the rationale for using ES over other methods. The use of dexamethasone by several of the aforementioned groups is one example of this, as emulsion-based encapsulation of dexamethasone can lead to low loading of the drug [128], whereas ES can lead to higher encapsulation efficiencies [41,120]. The vaccine adjuvants resiquimod [18,129] and cGAMP [48] are also examples where encapsulation efficiencies are poor with emulsion but increase with ES. In the cases of cGAMP and the adjuvant murabutide [45], the cell membrane partition coefficients of the adjuvants are exceedingly low, and therefore copious amounts of soluble drug are needed to permeate the cell's membrane (clinical trial #NCT02675439). Using ES to form particles that release their cargo intracellularly, the

barrier of the cell membrane is overcome. By identifying therapeutics that would partition into an aqueous phase easily, one can rationally maximize the benefits of ES formulation.

There are several areas of improvement for evaluating particle cytotoxicity, including assay selection, controls, selectivity of formulation, and concentration range. With regards to assays, many of the proposed studies focus on cytotoxicity measurements using a MTT based assay. With MTT-based assays, the number of mitochondria is measured, which can be an indicator of cell viability as well as proliferation. If the particles are of a small enough size, taking into consideration the polydispersity of the sample, they may be taken up by cells, slowing the cells' proliferation rate but not significantly affecting their viability. Earlier, our group did a study comparing viability as measured by an LDH assay and MTT assay [81]. We noted that there was significantly reduced viability as measured by MTT, but the LDH assay revealed very little toxicity. It was then hypothesized that engulfment of particles was likely the cause of the decreased MTT, which of course was reflected in a dose response fashion as observed with the MTT but not LDH assay (data not shown in manuscript). Although we did not conduct additional assays, we could have used a terminal deoxynucleotidyl transferase (TdT) dUTP Nick-End Labeling (TUNEL), or fluorescent live/dead assay to better evaluate cell viability. Several of the aforementioned papers used an LDH assay; however, other assays could be used to support the data found with the LDH assay. Additionally, when doing a cytotoxicity evaluation, drug-loaded and blank particles should both be used. Without the use of both blank and loaded particles, it is difficult to discern if observed cytotoxicity is the result of the carrier or the drug. To save samples, blank particles can just be used at the highest concentration. Finally, for chemotherapeutic studies, a selectivity of cytotoxicity in cancer *versus* non-cancer cells is preferred. Qu et al. [90] demonstrated this effect in their study, and it added to the understanding that with the ES formulation, drug is primarily affecting cancer cells over non-cancer cells. Also, to illustrate greater difference between soluble and encapsulated agents, a greater range of concentration is sometimes warranted, wherein low or high concentrations might lead to significant differences in either therapeutic effect or cytotoxicity. Controlled release systems can take longer to result in noticeable differences, so changes in concentration and time can make a significant difference in evaluating particles. Taken together, careful consideration of these aspects can improve the accuracy, quality and rigor of the cytotoxicity evaluation reported with ES or other particle systems.

Finally, the ES field will advance when more rigorous animal models are used for evaluation. For instance, orthotopic or spontaneous tumor models are considered more relevant than subcutaneous models. Orthotopic glioma models [130] in mice or rats would better mimic clinical standards for the disease and allow therapies to be more translatable. Similarly, more rigorous orthotopic models of triple negative breast cancer [131] would be the next step beyond subcutaneous models. Although these are challenging models, they can be accessed through collaboration and offer the potential to expand translational application of ES therapies.

5. Conclusion

As ES matures as a platform for generation of particle-based drug release systems, it is important to apply these systems in relevant *in vitro* and *in vivo* models. The work presented here on delivery of drugs, cells, genes, and vaccines, as well as tissue engineering, highlights the wonderful potential of this technology. As the application of ES progresses in the biomedical field, a greater impact of the work can also be realized through further optimization of the particles generated by the method and better choices of cargos, assays, and animal models.

Acknowledgements

NIH R01AI14133301 Micro-particle delivery of a potent intracellular adjuvant for a Universal Flu Vaccine *** NIH R41AI14079501 Advancing formulation of sting agonist for Universal Flu Vaccine **** NIH R01AI13752502 Biomaterials to study tolerance immune induction kinetics.

References

[1]. Nikolaou M, Krasia-Christoforou T, Eur. J. Pharm. Sci 113 (2018) 29–40. [PubMed: 28865687]

[2]. Qi S, Craig D, Adv. Drug Deliv. Rev 100 (2016) 67–84. [PubMed: 26776230]

[3]. Bachelder EM, Pino EN, Ainslie KM, Chem. Rev 117 (2017) 1915–1926. [PubMed: 28032507]

[4]. Farook U, Stride E, Edirisinghe MJ, Moaleji R, Med. Biol. Eng. Comput 45 (2007) 781–789. [PubMed: 17624564]

[5]. Wu Y, Duong A, Lee LJ, Wyslouzil BE, Electrospray Production of Nanoparticles for Drug/Nucleic Acid Delivery, Intech Europe, Rijeka, 2012.

[6]. Souva MS, Nabar GM, Winter JO, Wyslouzil BE, J. Colloid Interface Sci 512 (2018) 411–418. [PubMed: 29096101]

[7]. Duong AD, Ruan G, Mahajan K, Winter JO, Wyslouzil BE, Langmuir 30 (2014) 3939–3948. [PubMed: 24635446]

[8]. Sayed E, Karavasili C, Ruparelia K, Haj-Ahmad R, Charalambopoulou G, Steriotis T, Giasafaki D, Cox P, Singh N, Giassafaki LN, Mpenekou A, Markopoulou CK, Vizirianakis IS, Chang MW, Fatouros DG, Ahmad Z, J. Control. Release 278 (2018) 142–155. [PubMed: 29605567]

[9]. Collier MA, Bachelder EM, Ainslie KM, Pharm. Res 34 (2017) 419–426. [PubMed: 27896588]

[10]. Duong AD, Collier MA, Bachelder EM, Wyslouzil BE, Ainslie KM, Mol. Pharm 13 (2016) 92–99. [PubMed: 26568143]

[11]. Gallovic MD, Schully KL, Bell MG, Elberson MA, Palmer JR, Darko CA, Bachelder EM, Wyslouzil BE, Keane-Myers AM, Ainslie KM, Adv. Healthc. Mater 5 (20) (2016) 2617–2627. [PubMed: 27594343]

[12]. Corp R-HI., 1961.

[13]. Davoodi P, Feng F, Xu Q, Yan WC, Tong YW, Srinivasan MP, Sharma VK, Wang CH, J. Control. Release 205 (2015) 70–82. [PubMed: 25483422]

[14]. Leong KH, J. Aerosol Sci 18 (1987) 511–524.

[15]. Yao J, Lim LK, Xie J, Hua J, Wang CH, J. Aerosol Sci 39 (2008) 987–1002.

[16]. Almeria B, Deng W, Fahmy TM, Gomez A, J. Colloid Interface Sci 343 (2010) 125–133. [PubMed: 20022337]

[17]. Wang Y, Yang X, Liu W, Zhang F, Cai Q, Deng X, J. Microencapsul 30 (2013) 490–497. [PubMed: 23346923]

[18]. Duong AD, Sharma S, Peine KJ, Gupta G, Satoskar AR, Bachelder EM, Wyslouzil BE, Ainslie KM, Mol. Pharm 10 (2013) 1045–1055. [PubMed: 23320733]

[19]. Collier MA, Junkins RD, Gallovic MD, Johnson BM, Johnson MM, Macintyre AN, Sempowski GD, Bachelder EM, Ting JP, Ainslie KM, Mol. Pharm 15 (11) (2018) 4933–4946. [PubMed: 30281314]

[20]. Parhizkar M, Reardon PJT, Knowles JC, Browning RJ, Stride E, Pedley RB, Grego T, Edirisinghe M, Mater. Des 126 (2017) 73–84.

[21]. Lojewski B, Yang W, Duan H, Xu C, Deng W, Aerosol Sci. Technol 47 (2013) 146–152.

[22]. Johansen P, Martinez Gomez JM, Gander B, Expert Rev. Vaccines 6 (2007) 471–474. [PubMed: 17668999]

[23]. Paul WE, Fundamental Immunology, 4th ed., Raven Press, New York, 1994.

[24]. Xie J, Ng WJ, Lee LY, Wang CH, J. Colloid Interface Sci 317 (2008) 469–476. [PubMed: 17945246]

[25]. Davies LA, Hannavy K, Davies N, Pirrie A, Coffee RA, Hyde SC, Gill DR, Pharm. Res 22 (2005) 1294–1304. [PubMed: 16078139]

[26]. Chang PC, Chung MC, Lei C, Chong LY, Wang CH, J. Biomed. Mater. Res. A 100 (2012) 2970–2978. [PubMed: 22696306]

[27]. Jaworek A, Sobczyk AT, Krupa A, J. Aerosol Sci 125 (2018) 57–92.

[28]. Sengupta D, Das P, Mondal B, Mukherjee K, Renew. Sust. Energ. Rev 60 (2016) 356–376.

[29]. Jayaraman P, Gandhimathi C, Venugopal JR, Becker DL, Ramakrishna S, Srinivasan DK, Adv. Drug Deliv. Rev 94 (2015) 77–95. [PubMed: 26415888]

[30]. Kameoka J, Orth R, Ilic B, Czaplewski D, Wachs T, Craighead HG, Anal. Chem 74 (2002) 5897–5901. [PubMed: 12463378]

[31]. Chiarot PR, Sullivan P, Mrad RB, J. Microelectromech. Syst 20 (2011) 1241–1249.

[32]. Marijnissen J, Ciach T, Müller M, Winkels T, KB G, Schmidt-Ott A, Luding S, Experiment and simulation of electrospray particle-flows for controlled release of drugs, in: Hoogendoorn SP, Luding S, Bovy PHL, Schreckenberg M, Wolf DE (Eds.), Traffic and Granular Flow'03, Springer, Berlin, Heidelberg, 2005.

[33]. Boda SK, Li X, Xie J, J. Aerosol Sci 125 (2018) 164. [PubMed: 30662086]

[34]. Bock N, Dargaville TR, Woodruff MA, Prog. Polym. Sci 37 (2012) 1510–1551.

[35]. Mehta P, Haj-Ahmad R, Rasekh M, Arshad MS, Smith A, van der Merwe SM, Li X, Chang M-W, Ahmad Z, Drug Discov. Today 22 (2017) 157–165. [PubMed: 27693432]

[36]. Enayati M, Chang M-W, Bragman F, Edirisinghe M, Stride E, Colloids Surf. A Physicochem. Eng. Asp 382 (2011) 154–164.

[37]. Lu L, Peter SJ, Lyman MD, Lai HL, Leite SM, Tamada JA, Uyama S, Vacanti JP, Langer R, Mikos AG, Biomaterials 21 (2000) 1837–1845. [PubMed: 10919687]

[38]. Li L, Schwendeman SP, J. Control. Release 101 (2005) 163–173. [PubMed: 15588902]

[39]. Ding AG, Schwendeman SP, Pharm. Res 25 (2008) 2041–2052. [PubMed: 18622692]

[40]. Woodruff MA, D.W H, Prog. Polym. Sci 35 (2010) 1217–1256.

[41]. Carling CJ, Viger ML, Huu VA, Garcia AV, Almutairi A, Chem. Sci 6 (2015) 335–341. [PubMed: 25598962]

[42]. Broaders KE, Cohen JA, Beaudette TT, Bachelder EM, Frechet JM, Proc. Natl. Acad. Sci. U. S. A 106 (2009) 5497–5502. [PubMed: 19321415]

[43]. Reichard GA Jr., Haff AC, Skutches CL, Paul P, Holroyde CP, Owen OE, J. Clin. Invest 63 (1979) 619–626. [PubMed: 438326]

[44]. EPA, in: EPA (Ed.), www.epa.gov, 2005.

[45]. Chen N, Johnson MM, Collier MA, Gallovic MD, Bachelder EM, Ainslie KM, J. Control. Release 273 (2018) 147–159. [PubMed: 29407676]

[46]. Kauffman KJ, Do C, Sharma S, Gallovic MD, Bachelder EM, Ainslie KM, ACS Appl. Mater. Interfaces 4 (2012) 4149–4155. [PubMed: 22833690]

[47]. Kanthamneni N, Sharma S, Meenach SA, Billet B, Zhao JC, Bachelder EM, Ainslie KM, Int. J. Pharm 431 (2012) 101–110. [PubMed: 22548844]

[48]. Junkins R, Gallovic M, Johnson B, Collier M, Watkins-Schulz R, Cheng N, David C, McGee C, Sempowski G, Shterev I, McKinnone K, Bachelder E, Ainslie K, Ting J, Control J. Release 21 (2017) 1–13.

[49]. Thakral S, Thakral NK, Majumdar DK, Expert Opin. Drug Deliv 10 (2013) 131–149. [PubMed: 23102011]

[50]. Lee KY, Mooney DJ, Prog. Polym. Sci 37 (2012) 106–126. [PubMed: 22125349]
[51]. Hollabaugh CB, Burt LH, Walsh AP, Industrial & Engineering Chemistry 37 (1945) 943–947.
[52]. Chassard C, Delmas E, Robert C, Bernalier-Donadille A, FEMS Microbiol. Ecol 74 (2010) 205–213. [PubMed: 20662929]
[53]. Shokri J, Adibkia K, Application of cellulose and cellulose derivatives in pharmaceutical industries, in: Godbout T.v.d.V.a.L.(Ed.), Cellulose-medical, Pharmaceutical and Electronic Applications, IntechOpen, 2013.
[54]. Stankus JJ, Guan J, Fujimoto K, Wagner WR, Biomaterials 27 (2006) 735–744. [PubMed: 16095685]
[55]. Ullm S, Kruger A, Tondera C, Gebauer TP, Neffe AT, Lendlein A, Jung F, Pietzsch J, Biomaterials 35 (2014) 9755–9766. [PubMed: 25199786]
[56]. Zhu S, Huang M, Feng G, Miao Y, Wu H, Zeng M, Lo YM, Food Science & Nutrition 6 (2018) 1023–1031. [PubMed: 29983966]
[57]. Kuijpers AJ, van Wachem PB, van Luyn MJ, Plantinga JA, Engbers GH, Krijgsveld J, Zaat SA, Dankert J, Feijen J, J. Biomed. Mater. Res 51 (2000) 136–145. [PubMed: 10813755]
[58]. Barak S, Mudgil D, Khatkar BS, Crit. Rev. Food Sci. Nutr 55 (2015) 357–368. [PubMed: 24915383]
[59]. Helmerhorst EJ, Zamakhchari M, Schuppan D, Oppenheim FG, PLoS One 5 (2010).
[60]. Qi Y, Wang H, Wei K, Yang Y, Zheng RY, Kim IS, Zhang KQ, Int. J. Mol. Sci (2017) 18.
[61]. Shriner RL, Nabenhauer FP, Anderson RJ, J. Am. Chem. Soc 49 (1927) 1290–1294.
[62]. Van Laere KMJ, Hartemink R, Bosveld M, Schols HA, Voragen AGJ, Agric J. Food Chem. 48 (2000) 1644–1652.
[63]. Koukiekolo R, Cho H-Y, Kosugi A, Inui M, Yukawa H, Doi RH, Appl. Environ. Microbiol 71 (2005) 3504. [PubMed: 16000754]
[64]. Rose DJ, Patterson JA, Hamaker BA, Agric J. Food Chem. 58 (2010) 493–499.
[65]. Suksamran T, Ngawhirunpat T, Rojanarata T, Sajomsang W, Pitaksuteepong T, Opanasopit P, Int. J. Pharm 448 (2013) 19–27. [PubMed: 23524125]
[66]. Kean T, Thanou M, Adv. Drug Deliv. Rev 62 (2010) 3–11. [PubMed: 19800377]
[67]. Bellich B, D'Agostino I, Semeraro, Gamini A, Cesaro A, Marine Drugs 14 (2016).
[68]. Qiao D, Tu W, Liao A, Li N, Zhang B, Jiang F, Zhong L, Zhao S, Zhang L, Lin Q, Carbohydr. Polym 1 (2019) 199–207.
[69]. Vancha AR, Govindaraju S, Parsa KV, Jasti M, Gonzalez-Garcia M, Ballestero RP, BMC Biotechnol. 4 (2004) 23. [PubMed: 15485583]
[70]. Zeles-Hahn MG, Lentz YK, Anchordoquy TJ, Lengsfeld CS, J. Electrost 69 (2011) 67–77.
[71]. Lee MC, Seonwoo H, Garg P, Jang KJ, Pandey S, Kim HB, Park SB, Ku JB, Kim JH, Lim KT, Chung JH, RSC Adv. 8 (2018) 6452–6459. [PubMed: 35540421]
[72]. Wen Y, Pan S, Luo X, Zhang X, Zhang W, Feng M, Bioconjug. Chem 20 (2009) 322–332. [PubMed: 19152330]
[73]. Zhong Z, Ji Q, Zhang JA, J. Pharm. Biomed. Anal 51 (2010) 947–951. [PubMed: 19896790]
[74]. Simoes S, Filipe A, Faneca H, Mano M, Penacho N, Duzgunes N, Pedroso de Lima M, Expert Opinion on Drug Delivery 2 (2005) 237–254. [PubMed: 16296751]
[75]. Varshosaz J, Ghassami E, Noorbakhsh A, Jahanian-Najafabadi A, Minaiyan M, Behzadi R, Drug Dev. Ind. Pharm 44 (2018) 1012–1022. [PubMed: 29347846]
[76]. McSweeney MD, Versfeld ZC, Carpenter DM, Lai SK, Clin. Transl. Sci 11 (2018) 162–165. [PubMed: 29383836]
[77]. Rudmann DG, Alston JT, Hanson JC, Heidel S, Toxicol. Pathol 41 (7) (2013) 970–983. [PubMed: 23788571]
[78]. Webster R, Didier E, Harris P, Siegel N, Stadler J, Tilbury L, Smith D, Drug Metab. Dispos 35 (2007) 9–16. [PubMed: 17020954]
[79]. Cao Y, Liu F, Chen Y, Yu T, Lou D, Guo Y, Li P, Wang Z, Ran H, Sci. Rep 7 (2017) 11913. [PubMed: 28931908]

[80]. Furtmann B, Tang J, Kramer S, Eickner T, Luderer F, Fricker G, Gomez A, Heemskerk B, Jahn PS, J. Pharm. Sci 106 (2017) 3316–3327. [PubMed: 28652156]

[81]. Chen N, Collier MA, Gallovic MD, Collins GC, Sanchez CC, Fernandes EQ, Bachelder EM, Ainslie KM, Int. J. Pharm 512 (2016) 147–157. [PubMed: 27543351]

[82]. Ding L, Lee T, Wang CH, J. Control. Release 102 (2005) 395–413. [PubMed: 15653160]

[83]. Xie J, Marijnissen JC, Wang CH, Biomaterials 27 (2006) 3321–3332. [PubMed: 16490248]

[84]. Kumar Naraharisetti P, Yung Sheng Ong B, Wei Xie J, Kam Yiu Lee T, Wang CH, Sahinidis NV, Biomaterials 28 (2007) 886–894. [PubMed: 17067667]

[85]. Ranganath SH, Kee I, Krantz WB, Chow PK, Wang CH, Pharm. Res 26 (2009) 2101–2114. [PubMed: 19543956]

[86]. Hayashi K, Ono K, Suzuki H, Sawada M, Moriya M, Sakamoto W, Yogo T, Small 6 (2010) 2384–2391. [PubMed: 20878793]

[87]. Nie H, Fu Y, Wang CH, Biomaterials 31 (2010) 8732–8740. [PubMed: 20709388]

[88]. Gulfam M, Kim JE, Lee JM, Ku B, Chung BH, Chung BG, Langmuir 28 (2012) 8216–8223. [PubMed: 22568862]

[89]. Cao Y, Wang B, Wang Y, Lou D, RSC Adv. 4 (2014) 30430–30439.

[90]. Qu J, Liu Y, Yu Y, Li J, Luo J, Li M, Mater. Sci. Eng. C Mater. Biol. Appl 44 (2014) 166–174. [PubMed: 25280693]

[91]. Ramachandran R, Malarvizhi GL, Chandran P, Gupta N, Menon D, Panikar D, Nair S, Koyakutty M, J. Biomed. Nanotechnol 10 (2014) 1401–1415. [PubMed: 25016641]

[92]. Yin D, Yang Y, Cai H, Wang F, Peng D, He L, Mol. Pharm 11 (2014) 4107–4117. [PubMed: 25290462]

[93]. Zhang M, Tang Y, Zhu Z, Zhao H, Yao J, Sun D, J. Biomater. Sci. Polym. Ed 29 (2018) 1949–1963. [PubMed: 29920151]

[94]. Watkins-Schulz R, Tiet P, Gallovic MD, Junkins RD, Batty C, Bachelder EM, Ainslie KM, Ting JPY, Biomaterials 205 (2019) 94–105. [PubMed: 30909112]

[95]. Danhier F, Control J. Release 244 (2016) 108–121.

[96]. Marabelle A, Tselikas L, de Baere T, Houot R, Ann. Oncol 28 (2017) xii33–xii43. [PubMed: 29253115]

[97]. Solorio L, Patel RB, Wu H, Krupka T, Exner AA, Ther. Deliv 1 (2010) 307–322. [PubMed: 22816134]

[98]. Adamson C, Kanu OO, Mehta AI, Di C, Lin N, Mattox AK, Bigner DD, Expert Opin. Investig. Drugs 18 (2009) 1061–1083.

[99]. Grossman SA, Reinhard C, Colvin OM, Chasin M, Brundrett R, Tamargo RJ, Brem H, J. Neurosurg 76 (1992) 640–647. [PubMed: 1545259]

[100]. Arifin DY, Lee KY, Wang CH, J. Control. Release 137 (2009) 203–210. [PubMed: 19376172]

[101]. Arifin DY, Lee KY, Wang CH, Smith KA, Pharm. Res 26 (2009) 2289–2302. [PubMed: 19639394]

[102]. Lai W-F, Susha AS, Rogach AL, Wang G, Huang M, Hu W, Wong W-T, RSC Adv. 7 (2017) 44482–44491.

[103]. Mai Z, Chen J, He T, Hu Y, Dong X, Zhang H, Huang W, Ko F, Zhou W, RSC Adv. 7 (2017) 1724–1734.

[104]. Bayramov DF, Neff JA, Adv. Drug Deliv. Rev 112 (2017) 48–60. [PubMed: 27496704]

[105]. Hao S, Wang Y, Wang B, Deng J, Liu X, Liu J, Mater. Sci. Eng. C Mater. Biol. Appl 33 (2013) 4562–4567. [PubMed: 24094160]

[106]. Hao S, Wang Y, Wang B, Deng J, Zhu L, Cao Y, Mater. Sci. Eng. C Mater. Biol. Appl 39 (2014) 113–119. [PubMed: 24863206]

[107]. Hao S, Wang B, Wang Y, Xu Y, J. Nanopart. Res 16 (2014) 2204.

[108]. Paz-Samaniego R, Rascón-Chu A, Brown-Bojorquez F, Carvajal-Millan E, Pedroza-Montero M, Silva-Campa E, Sotelo-Cruz N, López-Franco YL, Lizardi-Mendoza J, J. Appl. Polym. Sci 135 (2018) 46411.

[109]. Ainslie KM, Lowe RD, Beaudette TT, Petty L, Bachelder EM, Desai TA, Small 5 (2009) 2857–2863. [PubMed: 19787677]

[110]. Stubelius A, Sheng W, Lee S, Olejniczak J, Guma M, Almutairi A, Small 14 (2018) e1800703. [PubMed: 30009516]

[111]. Xing Z, Zhang C, Zhao C, Ahmad Z, Li JS, Chang MW, Eur. J. Pharm. Sci 125 (2018) 64–73. [PubMed: 30248388]

[112]. Doavi T, Mousavi SL, Kamali M, Amani J, Ramandi MF, Iran. Biomed. J (2016) 20.

[113]. Manolova V, Flace A, Bauer M, Schwarz K, Saudan P, Bachmann MF, Eur. J. Immunol 38 (2008) 1404–1413. [PubMed: 18389478]

[114]. Wang F, Li Z, Tamama K, Sen CK, Guan J, Biomacromolecules 10 (2009) 2609–2618. [PubMed: 19689108]

[115]. Chang PC, Lim LP, Chong LY, Dovban AS, Chien LY, Chung MC, Lei C, Kao MJ, Chen CH, Chiang HC, Kuo YP, Wang CH, J. Dent. Res 91 (2012) 618–624. [PubMed: 22496127]

[116]. Nath SD, Son S, Sadiasa A, Min YK, Lee BT, Int. J. Pharm 443 (2013) 87–94. [PubMed: 23291448]

[117]. Chang PC, Chong LY, Dovban AS, Lim LP, Lim JC, Kuo MY, Wang CH, Tissue Eng Part A 20 (2014) 356–364. [PubMed: 23980713]

[118]. Zhao S, Agarwal P, Rao W, Huang H, Zhang R, Liu Z, Yu J, Weisleder N, Zhang W, He X, Integr. Biol. (Camb) 6 (2014) 874–884. [PubMed: 25036382]

[119]. Zamani M, Prabhakaran MP, Thian ES, Ramakrishna S, J. Colloid Interface Sci 451 (2015) 144–152. [PubMed: 25897850]

[120]. Gandhimathi C, Edwin NXH, Jayaraman P, Venugopal JR, Ramakrishna S, Kumar SD, Journal of Drug Metabolism & Toxicology (2015) 1–7.

[121]. Wang Y, Wei Y, Zhang X, Xu M, Liu F, Ma Q, Cai Q, Deng X, Chem. Eng. J 273 (2015) 490–501.

[122]. Esfahani RR, Jun H, Rahmani S, Miller A, Lahann J, ACS Omega 2 (2017) 2839–2847. [PubMed: 30023677]

[123]. Chang HC, Yang C, Feng F, Lin FH, Wang CH, Chang PC, J. Formos. Med. Assoc 116 (2017) 973–981. [PubMed: 28256366]

[124]. Link PA, Ritchie AM, Cotman GM, Valentine MS, Dereski BS, Heise RL, Tissue Eng J. Regen. Med 12 (2018) 2331–2336.

[125]. Zong H, Xia X, Liang Y, Dai S, Alsaedi A, Hayat T, Kong F, Pan JH, Mater. Sci. Eng. C Mater. Biol. Appl 92 (2018) 1075–1091. [PubMed: 30184730]

[126]. Soares RMD, Siqueira NM, Prabhakaram MP, Ramakrishna S, Mater. Sci. Eng. C Mater. Biol. Appl 92 (2018) 969–982. [PubMed: 30184827]

[127]. Park JB, Med. Oral Patol. Oral Cir. Bucal 14 (2009) e485–e488. [PubMed: 19415061]

[128]. Peine KJ, Guerau-de-Arellano M, Lee P, Kanthamneni N, Severin M, Probst GD, Peng HY, Yang YH, Vangundy Z, Papenfuss TL, LovettRacke AE, Bachelder EM, Ainslie KM, Mol. Pharm 11 (2014) 828–835. [PubMed: 24433027]

[129]. Schully KL, Sharma S, Peine KJ, Pesce J, Elberson MA, Fonseca ME, Prouty AM, Bell MG, Borteh H, Gallovic M, Bachelder EM, Keane-Myers A, Ainslie KM, Pharm. Res 30 (2013) 1349–1361. [PubMed: 23354770]

[130]. Graham-Gurysh E, Moore KM, Satterlee AB, Sheets KT, Lin FC, Bachelder EM, Miller CR, Hingtgen SD, Ainslie KM, Mol. Pharm 15 (2018) 1309–1318. [PubMed: 29342360]

[131]. Cheng N, Watkins-Schulz R, Junkins RD, David CN, Johnson BM, Montgomery SA, Peine KJ, Darr DB, Yuan H, McKinnon KP, Liu Q, Miao L, Huang L, Bachelder EM, Ainslie KM, Ting JP, JCI Insight (2018) 3.

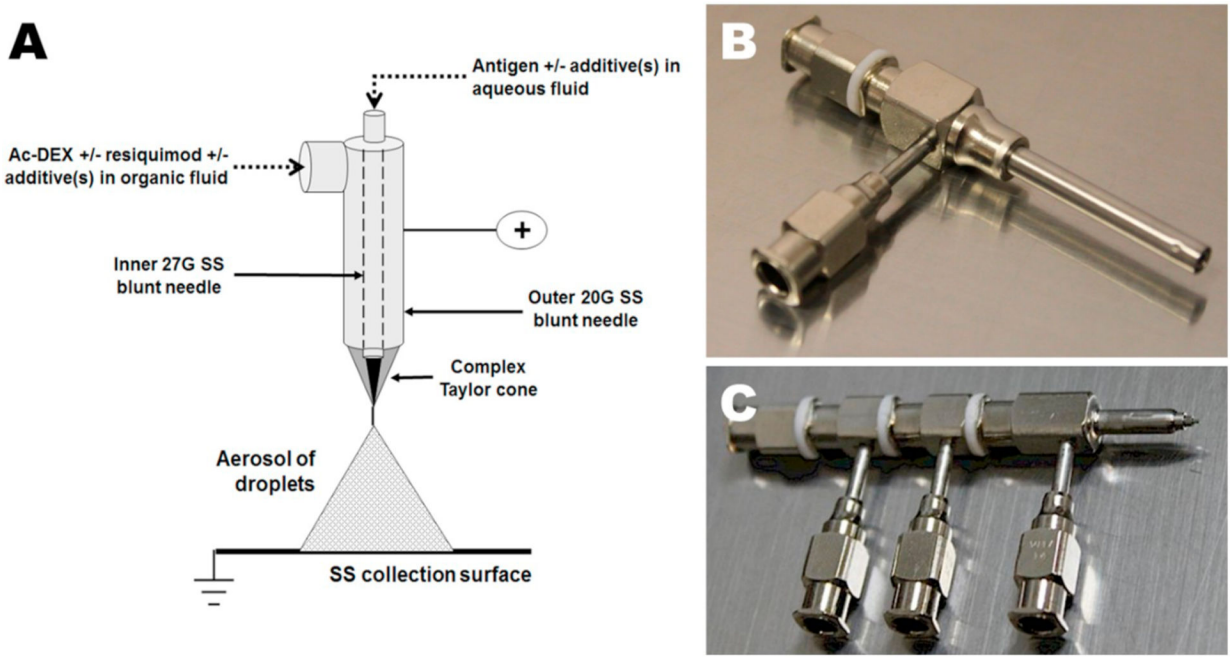

Fig. 1.

(A) Co-axial ES apparatus for generation of acetalated dextran (Ac-DEX) microparticles encapsulating the adjuvant resiquimod and a protein antigen in a single microparticle [11]. (B) Co-axial needle [12] and (C) Tetra-axial needle [12]. The Taylor cone would be created at the right-hand tip, with Luer-Lock style imports at the left and facing down.

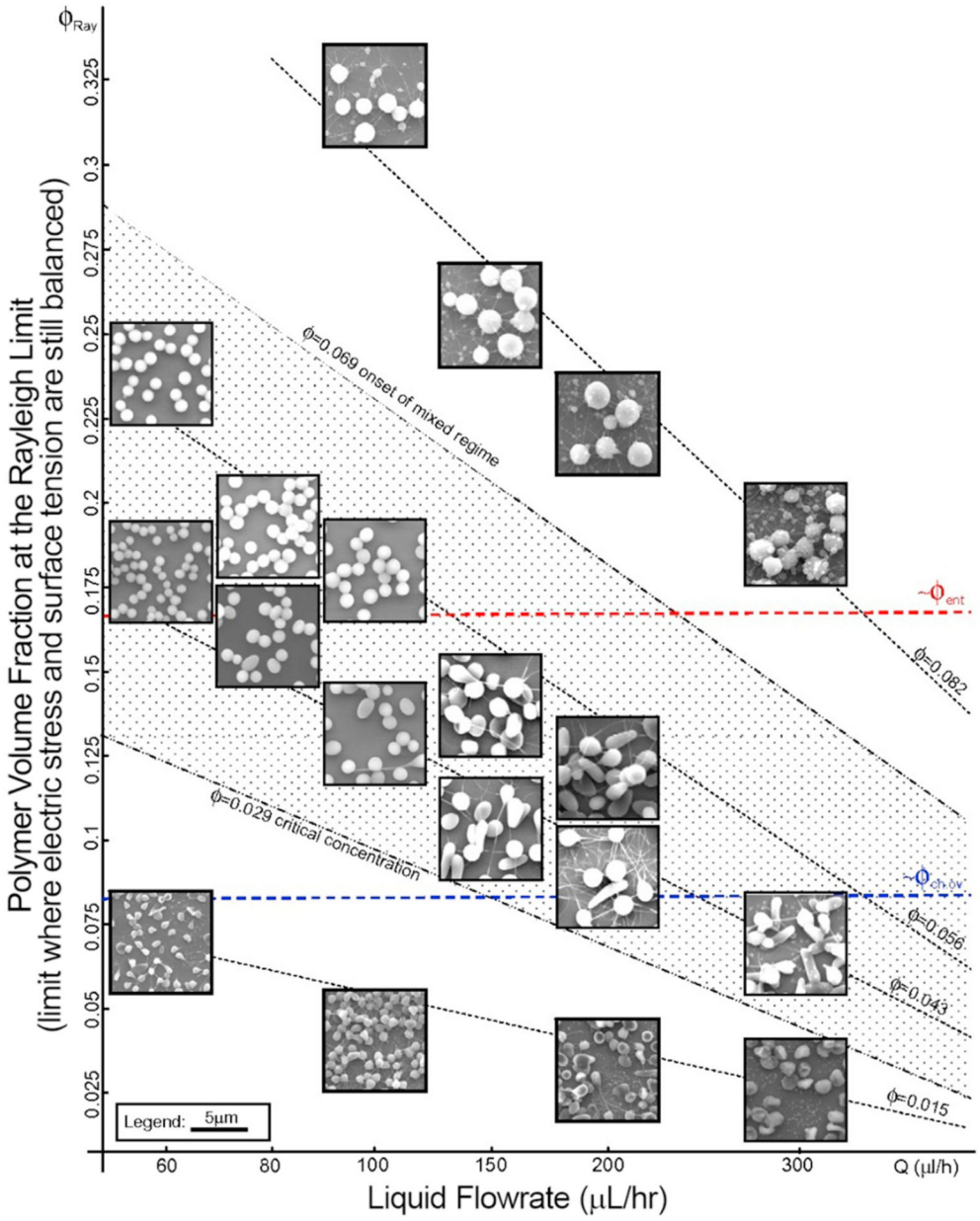

Fig. 2.

Figure modified from Almería et al. [16] to illustrate polydispersity of PLGA ES particles as a function of liquid flowrate (Q (μl/h)) and polymer volume fraction at the Rayleigh limit (ϕ). The Rayleigh limit is the point at which the electric stress and surface tension become unbalanced and the Taylor cone, or the flow in general, becomes unstable. Entanglement volume fraction, ϕ_{ent}, is the volume fraction of polymer within the droplet that is large enough to form an entangled network of polymer chains. The overlap volume fraction, $\phi_{ch.ov}$, is the polymer volume fraction where the average distance between chains is equivalent to their radius in solution.

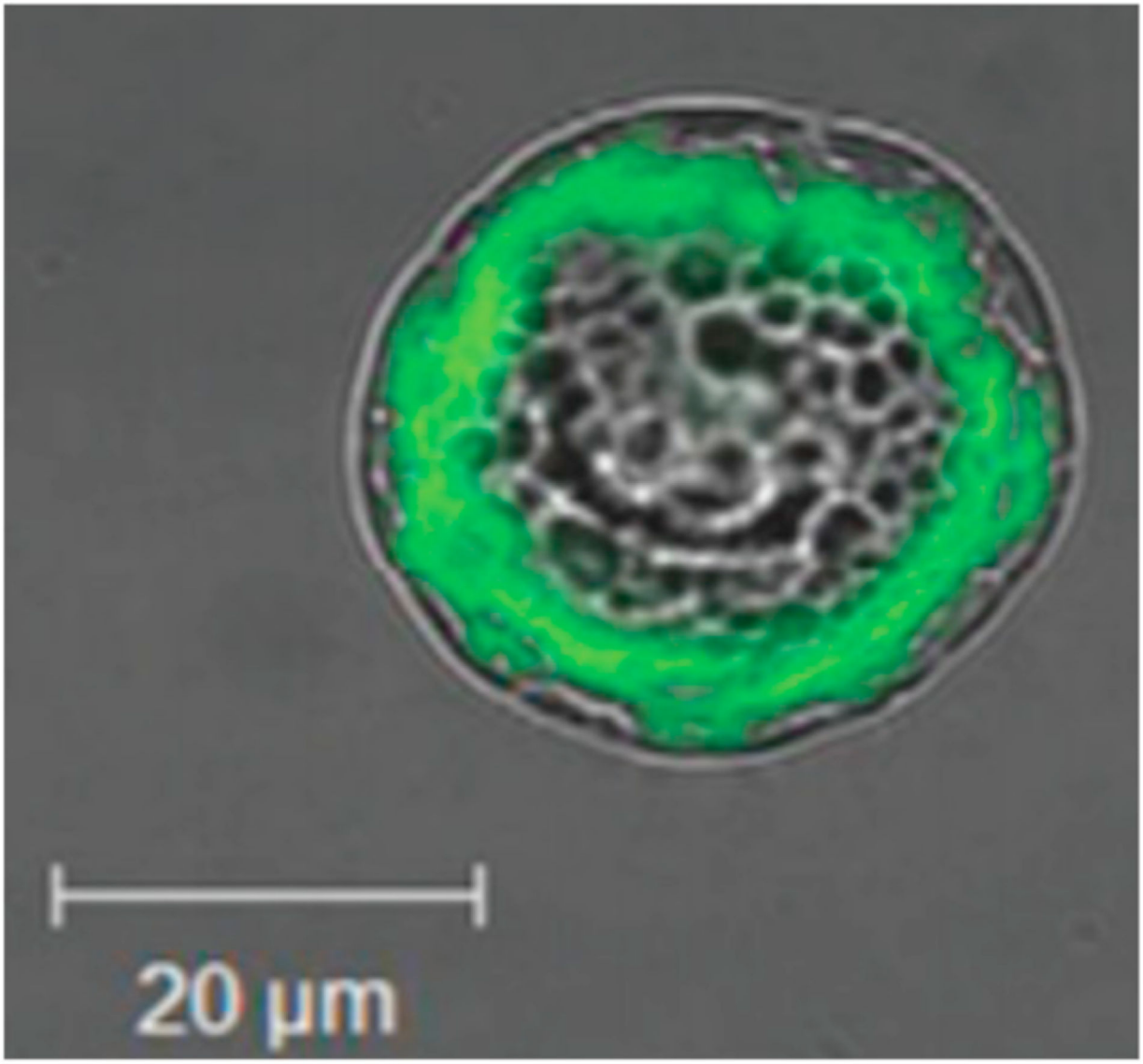

Fig. 3.

Fluorescent micrograph of coumarin-6 encapsulated in the core of a core-shell *co*-axial ES microparticle comprised of poly(D, L-lactide) and poly(D,L-lactide-*co*-glycolide) [26].

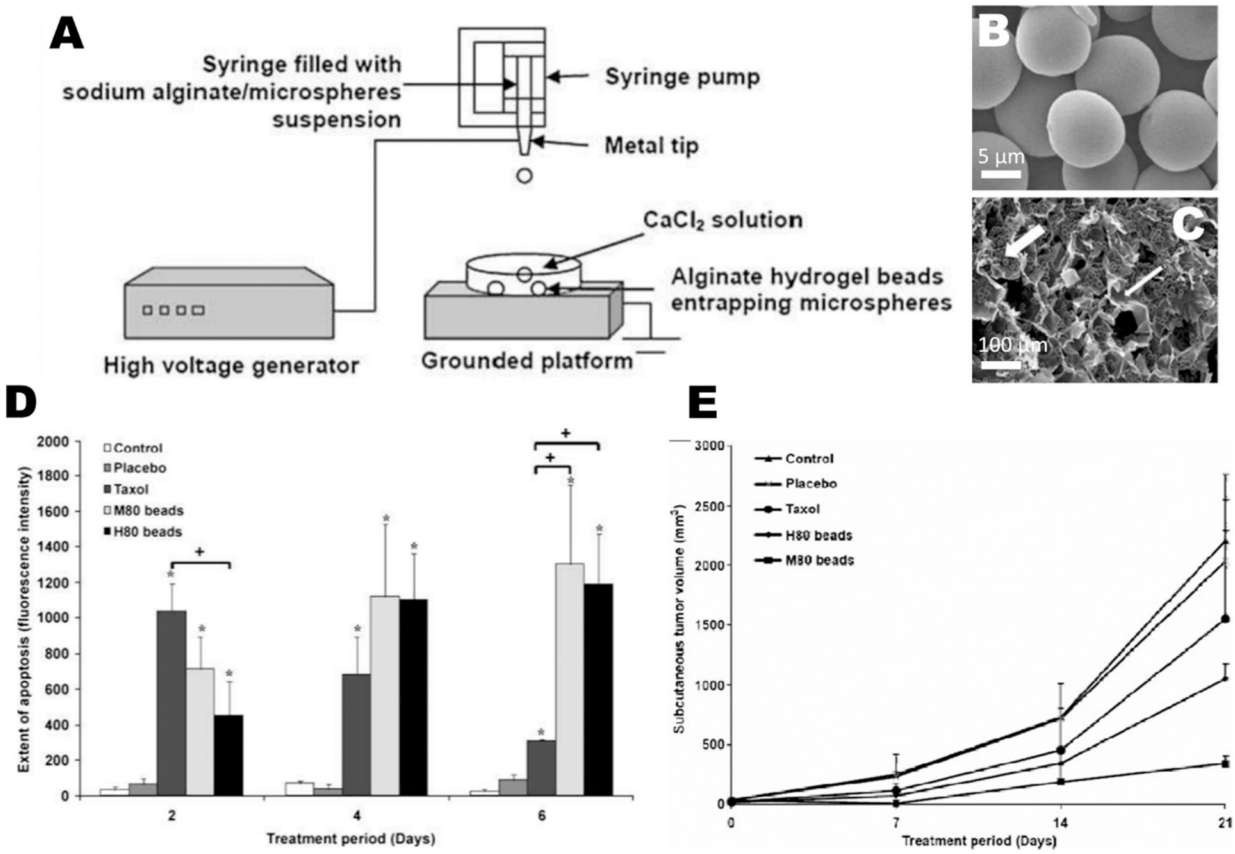

Fig. 4.

Ranganath et al.'s [85] encapsulation of ES paclitaxel PLGA particles in alginate (A-C), and then *in vitro* evaluation for apoptosis when cultured with C6 glioma cells (D) and when used peritumorally to treat a C6 subcutaneous tumor (E). Micrograph B is of the PLGA paclitaxel particles, and micrograph C is of the alginate particles, with the arrows indicating PLGA particles.

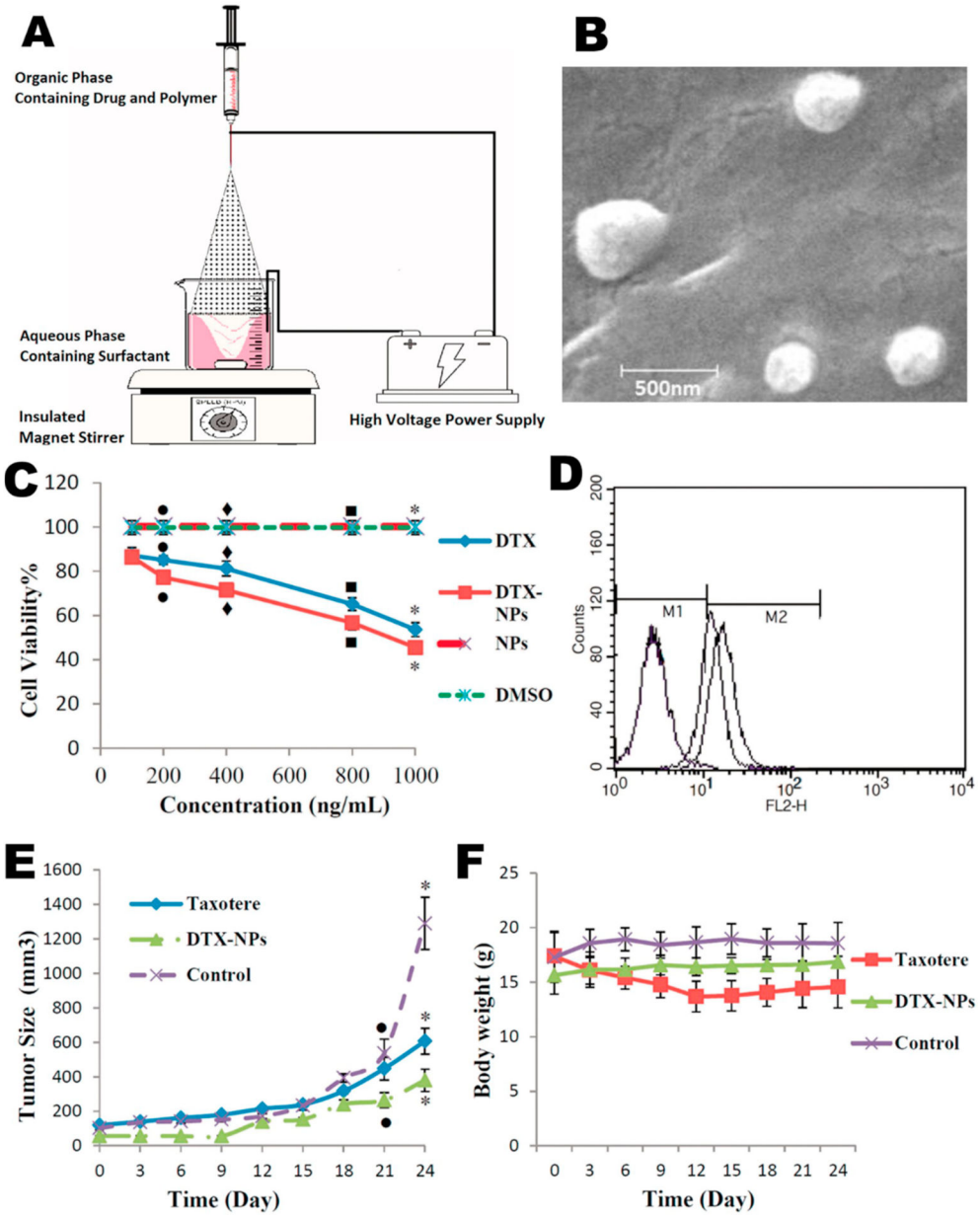

Fig. 5.

Varshosaz et al. [75] applied Ecoflex® and PEG particles encapsulating docetaxel for the *in vitro* and *in vivo* treatment of ovarian cancer. (A) They prepared their particles by spraying into an aqueous phase containing a surfactant to stabilize and prevent coalescence of sprayed particles. Note the necessity of insulating the magnetic stirrer from the high voltage of the spray apparatus. (B) SEM micrograph of particles formed. (C) Presents cell viability *in vitro* where DTX refers to docetaxel, and NP nanoparticles.(D) The uptake of particles labeled with rhodamine B, as measured by flow cytometry, where M1 indicates autofluorescence of blank cells and the M2 region indicates greater fluorescence due to particle uptake. Each of the three particle groups in the M2 region were treated with rhodamine-loaded particles while the group in the M1 region was treated with unloaded particles. (E) Size of

subcutaneous ovarian tumor with treatment of drug (Taxotere)-loaded particle, drug alone or with no treatment. (F) Body weight of each treatment group in E.

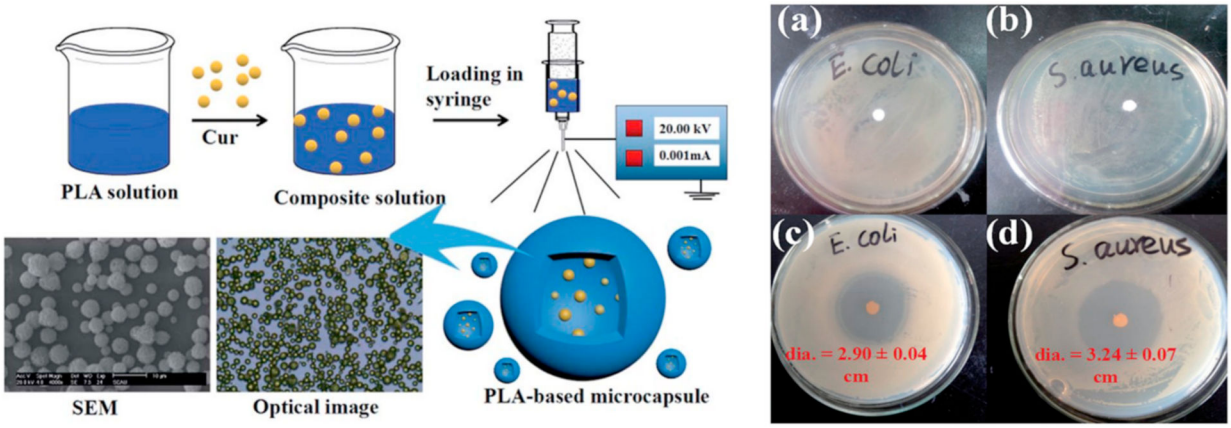

Fig. 6.

Fabrication by Mai et al. [103] of PLA particles encapsulating curcumin (left) with scale bar equal to 10 μm. Incubation of control particles (a–b) and curcumin loaded particles (c–d) with two different bacteria (right), demonstrating the effective inhibition of bacterial growth by the curcumin-loaded particles.

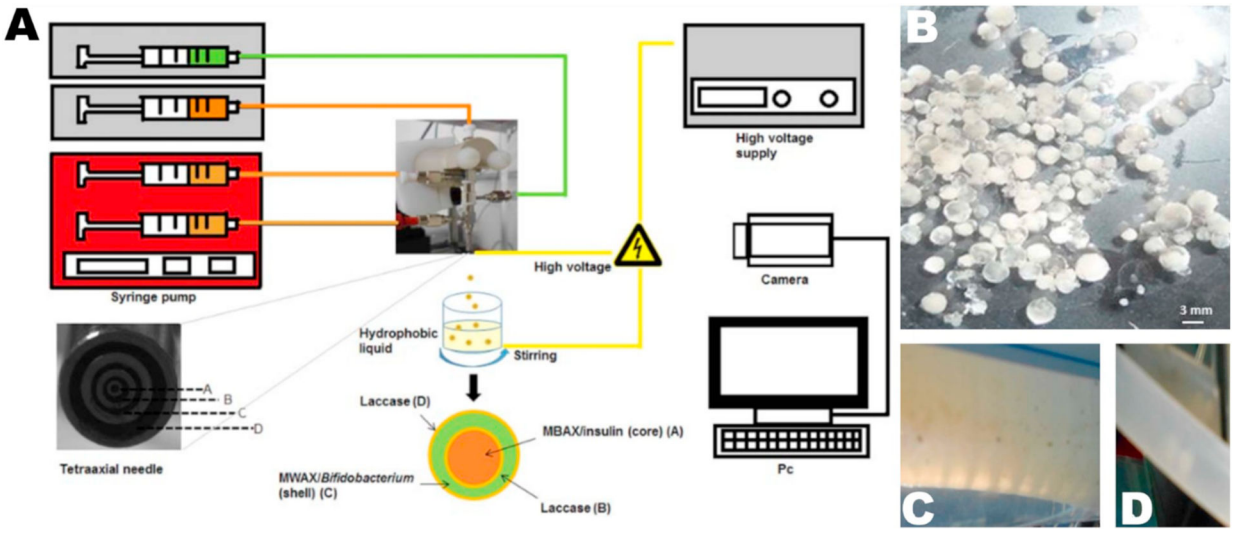

Fig. 7.

Paz-Samaniego et al. [108] generated ES particles from corn-based arabinoxylans to encapsulate bacteria and insulin *via* tetra-axial spraying (A). (B) Photograph of particles encapsulating two bacteria and insulin. Particles encapsulating insulin and bacteria in the stomach (C) and small intestine (D) compartments of the GI tract simulator Simgi®.

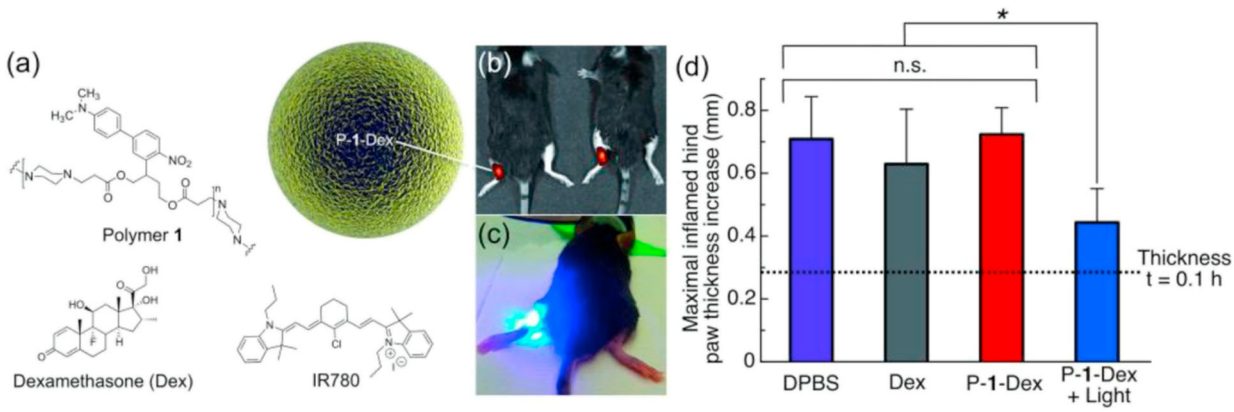

Fig. 8.

Carling et al. [41] applied 2-(40-*N*-dimethylamino-4-nitro-[1,10-biphenyl]-3-yl)butane-1,4-diyl dicarbonyl (Polymer 1) to encapsulate dexamethasone in ES particles (a). IR780 is a near IR fluorescent probe. (b) Illustrates location of injection on the mouse, with (c) showing application of light. In (d), Carrageenan-induced hind paw inflammation was induced and treated with either saline control (DPBS), dexamethasone (Dex) and dexamethasone encapsulated in Polymer 1, with or without subsequent near IR light stimulation (P-1-Dex and P-1-Dex + Light, respectively). Significant reduction in paw thickness increase was observed with the light-triggered release of dexamethasone from the particles.

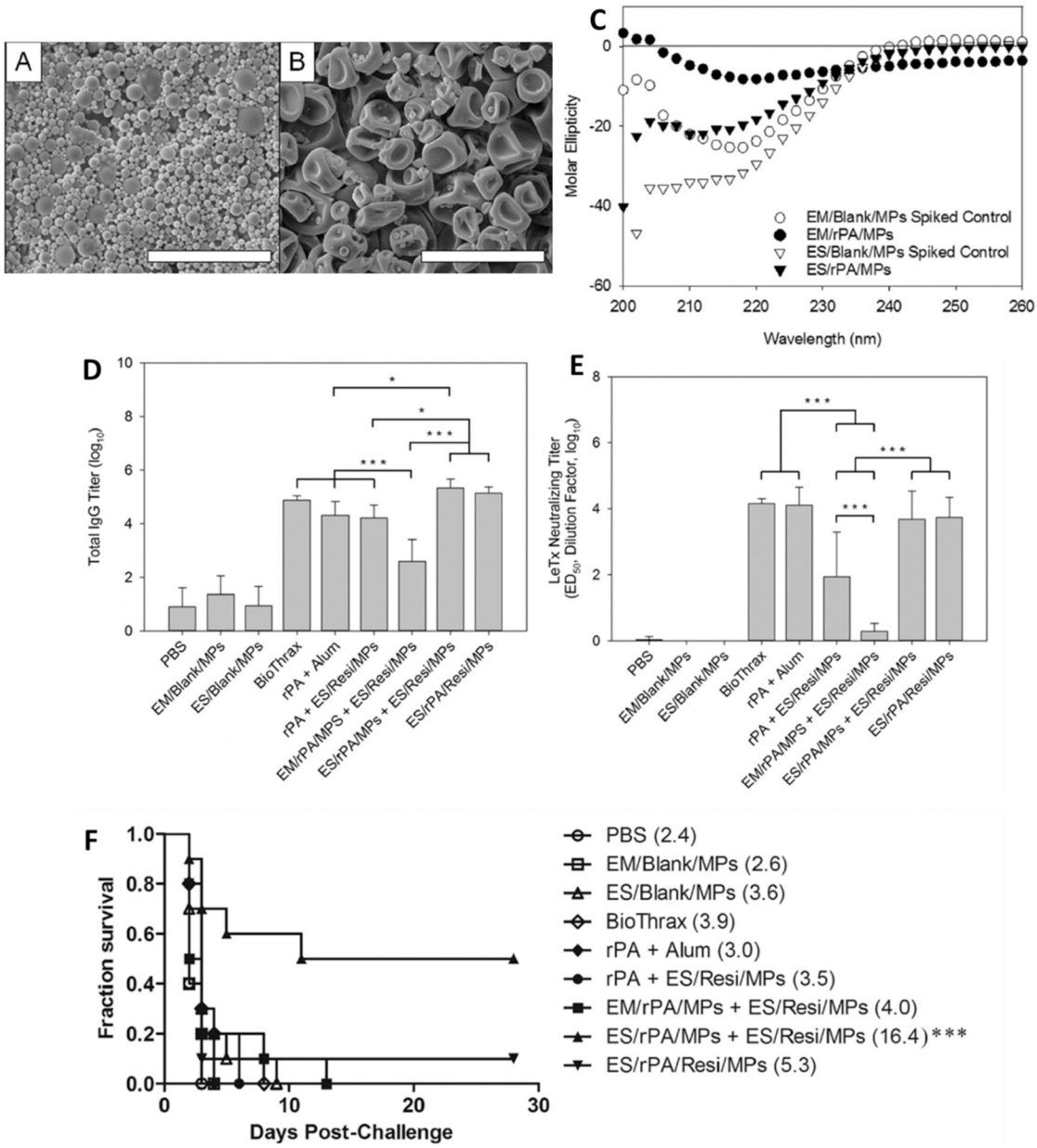

Fig. 9.

Gallovic et al. [11] ES of Ac-DEX to encapsulate rPA (PA) and resiquimod (Resi). Micrograph of (A) emulsion (EM) and (B) ES particles. (C) Circular dichroism of rPA from different particles and blank particles spiked with protein ideally stored. (D) Total serum IgG after vaccination with experimental groups. (E) Toxin neutralization of serum antibodies isolated from mice after vaccination. (F) Survival after vaccination and lethal challenge with different experimental groups.

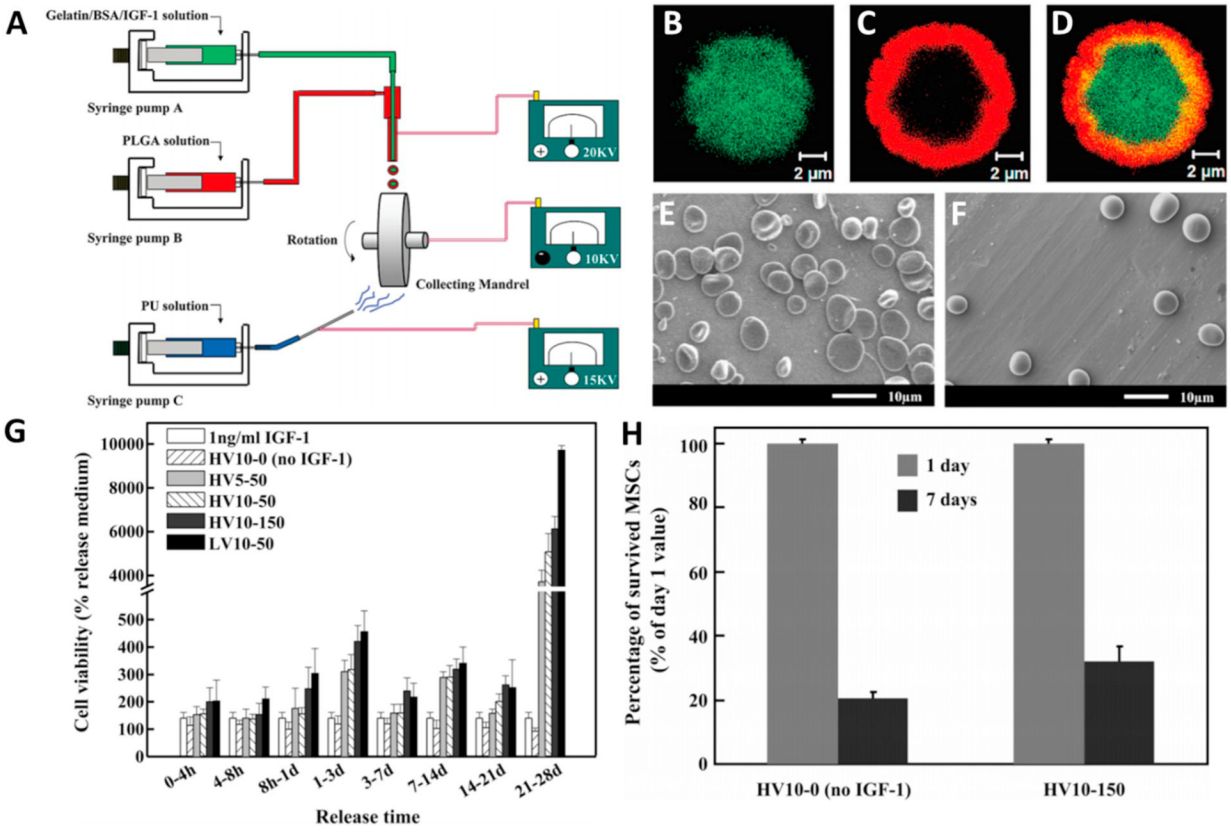

Fig. 10.

Wang et al. [114] combined spraying and aligned spinning apparatus to create particle-laden electrosprayed scaffolds (A). (B–D) Rhodamine-B loaded PLGA (red) shell and FITC-BSA (green) loaded core. Scanning electron micrograph of (E) 5% and (F) 10% IGF-1 loaded PLGA particles. (G) Bioactivity of IGF-1 released on SMCs. HV stands for high molecular weight, and LV low molecular weight. The numbers refer to loading of IGF-1 in μg/mL. (H) The percentage of surviving MSCs under hypoxic conditions and nutrient starvation conditions.

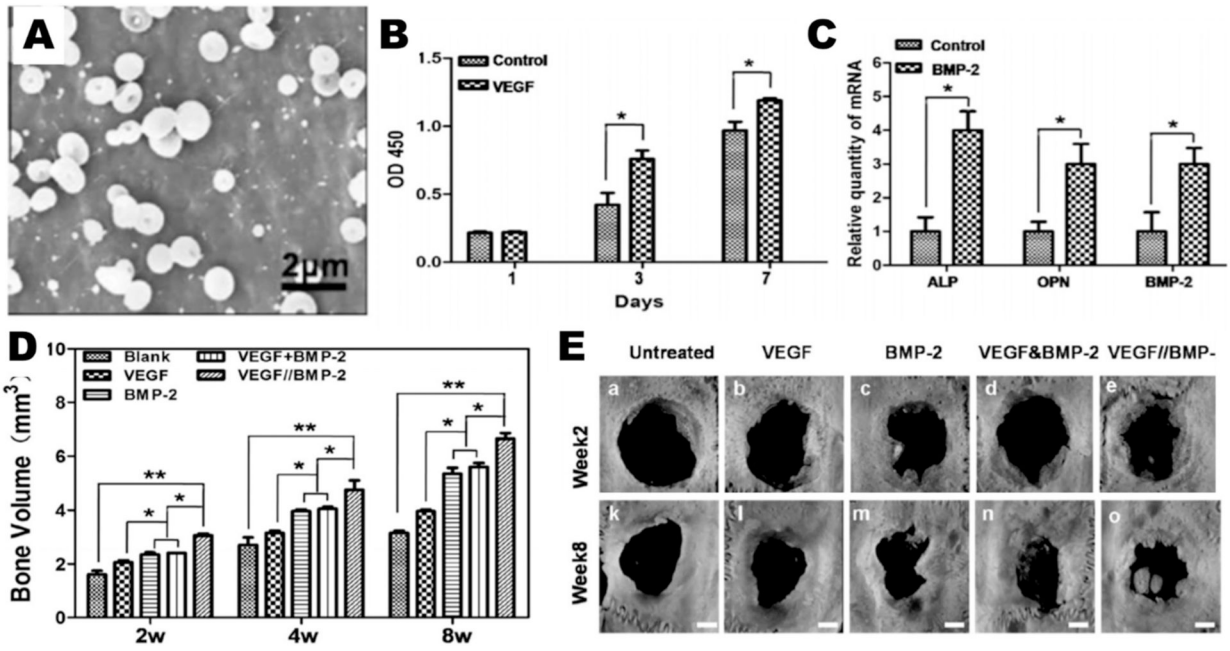

Fig. 11.

Wang et al. [121] used PLGA and PLA to particles to encapsulate VEGF and BMP-2. (A) Scanning electron micrograph of ES particles. (B) Proliferation of MECs when cultured with VEGF loaded particles. (C) RT-PCR was used to report gene expression profiles of ALP, OPN, and BMP-2 on day 14 Following treatment with BMP-2 loaded particles. (D, E) Bone volume measured by 3D μ-CT of rat calvarial bone defects treated with different groups, and images of osteotomies in each group at 2 and 8 weeks after treatment.

Table 1

Summary of matrices used in electrospray for drug delivery.

Polymer class	Polymer	Degradation mechanism	Degradation rate	Degradation by-products	Ref
Polyesters	Poly(lactic acid) (PLA)	Hydrolysis of ester bonds	Months	Lactic acid	[37–39]
	Poly(glycolic acid) (PGA)			Glycolic acid	[37–39]
	Poly(lactic-co-glycolic acid) (PLGA)			Lactic acid and glycolic acid	[37–39]
	Polycaprolactone (PCL)			Caproic acid	[37,40]
Stimuli responsive	2-(40-*N*-dimethylamino-4-nitro-[1,10-biphenyl]-3-yl)butane-l,4-diyl dicarbonyl	Light responsive	Minutes when exposed to visible light (λ_{ex} = 400–500 nm)	Photocleaved nitro-alkene derivative; secondary products not yet identified	[41]
	Acetalated Dextran (Ac-DEX; Ace-DEX)	Hydrolysis of acetal groups	Tunable, ranging from hours to months based on reaction time and molecular weight	Dextran and exceedingly low levels of acetone and a short chain alcohol	[3,42–48]
	Eudagrits (methacrylic acid and methyl methacrylate *co*-polymers)	Not biodegradable	–	–	[49]
Natural polymers	Alginate	Not biodegradable	–	–	[50]
	Cellulose Derivatives	Hydrolysis and cellulases	Varies	Glucose; other degradation products vary by derivatives	[51–53]
	Gelatin	Hydrolysis and enzymatic degradation	Weeks or months	Prolylhydroxyproline and glycine	[54–57]
	Gliadin	Proteases	Slow: can be resistant to digestion	Glutamine and proline residues	[58,59]
	Fibroin	Not biodegradable	–	–	[60]
	Maize arabinoxylans	Enzymatic degradation by gut resident microbes	De-branching occurs on the order of days	Arabinose and xylose	[61–64]
	Chitosan	Enzymatic degradation	Varies based on degree of deacetylation and molecular weight	Glucosamine and chito-oligosaccharides	[65–67]
	Starches from yams	Hydrolysis and enzymatic degradation	Hours	Amylose and Amylopectin	[65,68]
Cationic polymer and lipid	Poyethylenimine (PEI)	Non-biodegradable	–	–	[69–72]
	1,2-dioleoyl-3-trimethylammonium-propane (DOTAP)	Hydrolysis of ester linkage		Unsaturated diacyl tails and amine head group	[70,73,74]
Other non-degradable	Ecoflex®	Non-biodegradable	–	–	[75]
polymers	Polyethylene glycol (PEG)		–	–	[76–78]
	Polyvinyl alcohol (PVA)		–	–	[79,80]

Table 2

Electrospray technologies developed for cancer drug delivery.

Polymer	Cargo	Axial	Particle size range	Cell model	Animal model	Ref
PCL	Taxol	Mono	1–15 μm	C6 Glioma	–	[82]
PLGA	Paclitaxel	Mono	200 nm-10 μm	C6 Glioma	–	[83]
PLGA	Paclitaxel	Mono	13–17 μm	–	C6 Glioma cells subQ (BALB/c nude mice)	[84]
PLGA+Alginate	Paclitaxel	Mono (two-step)	10–15 μm (post-first step) 1.6–1.7 mm (post-second step)	C6 Glioma	C6 Glioma cells subQ (BALB/c nude mice)	[85]
EHEC	Fe_3O_4 NPs	Mono	1–10 μm	GL261 Glioma	–	[86]
PLA PLGA	PaclitaxelSuramin	Co (miscible)	10–20 μm	U87 Glioma	U87 Glioma cells subQ (BALB/c nude mice)	[87]
Gliadin or Gliadin-Gelatin	Cyclophosphamide	Mono	200–400 nm	MCF7 Breast	–	[88]
PLGA+PCL or PVP	Combretastatin A4 Doxorubicin	Co (miscible)	400–500 nm	B16-F10 Melanoma HUVECs	–	[89]
Silk Fibroin	Cisplatin	Mono	59–75 nm	A549 Lung L929 Fibroblasts	–	[90]
PLGA+Albumin	(5,10,15, 20-tetrakis(mesohydroxyphenyl)porphyrin) (mTHPP), Dasatinib	Mono	80–90 nm	U87MG Glioma	No disease (Wistar rats)	[91]
PLA	Gambogic-acid	Mono	70–7500 nm	–	H22 cells orthotopic	[92]
Silk Fibroin PVA	Doxorubicin	Co (miscible)	300–1800 nm	MDA-MB-231 Breast	MDA-MB-231 cells subQ (BALB/c nude mice)	[79]
Ecoflex®PEG	Docetaxel	Mono	360 nm	SKOV-3 Ovarian	SKOV-3 cells subQ (B6 nude)	[75]
PLGA	Paclitaxel Etoposide	Co (miscible)	1–4 μm	Saos-2 Osteosarcoma	–	[93]
Ac-DEX	cGAMP	Co (semimiscible)	1–3 μm	BMDCs	B16F10 in C57BL/6 mice Orthotopic E077 in C57BL/6 and 6(Cg)-Tmem173tm1.2Camb/J (Tmem173−/−) mice	[94]

Table 3

Electrospray technologies for delivery of antimicrobial therapies.

Polymer	Cargo	Axial	Particle size range	Cell model	Animal model	Ref
Ac-DEX	Resiquimod	Mono	1–2 μm	RAW 264.7 Macrophages	Visceral Leishmaniasis (BALB/C mice)	[18]
CMC Alginate	Tetracycline hydrochloride	Mono	400–600 nm	3T3 Fibroblasts HEK293	–	[102]
PLA	Curcumin	Mono	1–20 μm	*E. coli* *S. aureus* HEK293T cells PC12 cells Human dermal fibroblasts	–	[103]

Table 4

Electrospray particle systems for oral delivery.

Polymer	Cargo	Axial	Particle size range	Cell model	Ref
Eudragit L 100–55	Omeprazole	Mono	200–350 nm	Caco-2 cells	[105]
PLGA	Metronidazole	Mono	1–8 μm	GES-1 cells	[106]
Eudragit L 100–55 Eudragit RS	Aspirin	Co (miscible)	280–435 nm	Caco-2 cells	[107]
Maize Bran Arabinoxylans Maize Wax Arabinoxylans	*Bifidobacterium longum* *B. adolescents* Insulin	Tetra (miscible)	2–3 μm	Simgi®	[108]

Table 5

Electrospray technologies for gene delivery.

Polymer	Cargo	Axial	Particle size range	Cell model	Animal model	Ref
PEI Poly L-lysine DOTAP	Luciferase plasmid DNA	Mono	N/A	Human Derived Tracheal/Bronchial Epithelial Cells (EpiAirway®)	–	[70]
PEI	DNA 3T3 fibroblasts	Mono	N/A	3T3 fibroblasts	–	[41,71]

Table 6

Electrospray technologies for treatment of inflammation and oxidative stress.

Polymer	Cargo	Axial	Particle size range	Cell model	Animal model	Ref
2-(40-*N*-dimethylamino-4-nitro- [1,1O-biphenyl] −3-yl)butane-l ,4-diyl dicarbonyl	Dexamethasone	Mono	1 μm	RAW 264.7 macrophages	Carrageenan-induced hind paw inflammation (C57BL/6 mice)	[41]
Ac-DEX PLGA	Dexamethasone	Mono	3.3 μm	Cl 66 Endothelial cells C57B1/6 Bone-marrow derived macrophages	Dermal air pouch (inflammation model) Monosodium urate crystal (Gout) model	[110]
PCL	Ganoderma lucidum polysaccharide	Tri	13.37 μm	MRC-5 human lung fibroblasts	Pathogen-free KunMing mice	[111]

Table 7

Electrospray technologies for vaccine delivery.

Polymer	Cargo	Axial	Particle size range	Cell model	Animal model	Ref
Alginate n-(4-*n,n*-dimethylaminocinnamyl) chitosan Yam starch	Ovalbumin	Mono	0.75–3μim	Caco-2 cells *ex vivo* Porcine Intestine	BALB/c mice	[65]
Chitosan Trimethylated Chitosan	Recombinant synthetic antigen EIT	Mono	300–600 nm	Caco-2 cells	BALB/c mice	[112]
Ac-DEX	rPA Resiquimod	Co (immiscible)	1–3 μm	_	BALB/c mice	[11]
Ac-DEX PLGA	cGAMP	Co (semi-miscible)	1–3 μm	BMDCs	C57BL/6 mice	[48]
Ac-DEX PLGA	cGAMP Resiquimod	Co (semi-miscible)				[19]
PLGA PVA	Cytomegalovirus (CMV) peptides pp65 & IE-1	Mono	150–800 nm	PBMCs	_	[80]
Ac-DEX	Ovalbumin Murabutide	Co (semi-miscible)	500–600 nm	JAWSII dendritic cells	C57BL/6 mice	[45]

Table 8

Electrospray technologies for tissue engineering.

Polymer	Cargo	Axial	Particle size range	Cell model	Animal model	Ref
PLGA Gelatin	Insulin-like growth factor	Co (immiscible)	5 μm	MSCs SMCs	–	[114]
PLA PLGA	PDGF Simvastatin	Co (semi-miscible)	15–20 μm	–	Osteotomy repair (Sprague-Dawley rats)	[115]
PLGA	Simvastatin	Mono	1.6–8 μm	MG-63 osteoblasts	–	[116]
PLA PLGA	PDGF Simvastatin	Co (semi-miscible)	18–21 μm	–	Osteotomy repair (Sprague-Dawley rats)	[117]
Alginate CMC	R1 Embryonic stem cells	Co (miscible)	285–345 μm	–	–	[118]
PLGA	BSA SDF-1α	Co (semi-miscible)	4 μm	MSCs	–	[119]
PCL Silk fibroin	Ascorbic acid Dexamethasone	Mono	0.7–8 μm	ADSCs	–	[120]
PLA PLGA	VEGF BMP-2	Co (semi-miscible)	0.5–1.5 μm	MECs BMSCs	Calvarial bone defects (Sprague-Dawley rats)	[121]
PLGA	3T3 fibroblasts	Co (immiscible)	~10 μm	–	–	[122]
PLGA	BMP-2	Co (semi-miscible	439 nm	–	Titanium screw implant model (Sprague-Dawley rats)	[123]